

1           A Fast and Scalable Framework for Large-scale and  
2           Ultrahigh-dimensional Sparse Regression with Application to  
3           the UK Biobank

4           Junyang Qian<sup>1</sup>, Yosuke Tanigawa<sup>2</sup>, Wenfei Du<sup>1</sup>, Matthew Aguirre<sup>2</sup>, Chris Chang<sup>3</sup>,  
5           Robert Tibshirani<sup>1,2</sup>, Manuel A. Rivas<sup>2</sup>, and Trevor Hastie<sup>1,2</sup>

6                           <sup>1</sup>Department of Statistics, Stanford University

7                           <sup>2</sup>Department of Biomedical Data Science, Stanford University

8                           <sup>3</sup>Grail, Inc.

9                           **Abstract**

10           The UK Biobank (Bycroft et al., 2018) is a very large, prospective population-based cohort  
11           study across the United Kingdom. It provides unprecedented opportunities for researchers to  
12           investigate the relationship between genotypic information and phenotypes of interest. Multiple  
13           regression methods, compared with GWAS, have already been showed to greatly improve the  
14           prediction performance for a variety of phenotypes. In the high-dimensional settings, the lasso  
15           (Tibshirani, 1996), since its first proposal in statistics, has been proved to be an effective method  
16           for simultaneous variable selection and estimation. However, the large scale and ultrahigh  
17           dimension seen in the UK Biobank pose new challenges for applying the lasso method, as many  
18           existing algorithms and their implementations are not scalable to large applications. In this  
19           paper, we propose a computational framework called batch screening iterative lasso (BASIL)  
20           that can take advantage of any existing lasso solver and easily build a scalable solution for very  
21           large data, including those that are larger than the memory size. We introduce **snpnet**, an R

22 package that implements the proposed algorithm on top of **glmnet** (Friedman et al., 2010a)  
23 and optimizes for single nucleotide polymorphism (SNP) datasets. It currently supports  $\ell_1$ -  
24 penalized linear model, logistic regression, Cox model, and also extends to the elastic net  
25 with  $\ell_1/\ell_2$  penalty. We demonstrate results on the UK Biobank dataset, where we achieve  
26 superior predictive performance on quantitative and qualitative traits including height, body  
27 mass index, asthma and high cholesterol.

## 28 Author Summary

29 With the advent and evolution of large-scale and comprehensive biobanks, there come up unprece-  
30 dented opportunities for researchers to further uncover the complex landscape of human genetics.  
31 One major direction that attracts long-standing interest is the investigation of the relationships  
32 between genotypes and phenotypes. This includes but doesn't limit to the identification of geno-  
33 types that are significantly associated with the phenotypes, and the prediction of phenotypic values  
34 based on the genotypic information. Genome-wide association studies (GWAS) is a very powerful  
35 and widely used framework for the former task, having produced a number of very impactful dis-  
36 coveries. However, when it comes to the latter, its performance is fairly limited by the univariate  
37 nature. To address this, multiple regression methods have been suggested to fill in the gap. That  
38 said, challenges emerge as the dimension and the size of datasets both become large nowadays.  
39 In this paper, we present a novel computational framework that enables us to solve efficiently the  
40 entire lasso or elastic-net solution path on large-scale and ultrahigh-dimensional data, and therefore  
41 make simultaneous variable selection and prediction. Our approach can build on any existing lasso  
42 solver for small or moderate-sized problems, scale it up to a big-data solution, and incorporate  
43 other extensions easily. We provide a package **snpnet** that extends the **glmnet** package in R and  
44 optimizes for large phenotype-genotype data. On the UK Biobank, we observe improved prediction  
45 performance on height, body mass index (BMI), asthma and high cholesterol by the lasso over other  
46 univariate and multiple regression methods. That said, the scope of our approach goes beyond ge-  
47 netic studies. It can be applied to general sparse regression problems and build scalable solution  
48 for a variety of distribution families based on existing solvers.

## 49 1 Introduction

50 The past two decades have witnessed rapid growth in the amount of data available to us. Many  
51 areas such as genomics, neuroscience, economics and Internet services are producing big datasets  
52 that have high dimension, large sample size, or both. A variety of statistical methods and computing  
53 tools have been developed to accommodate this change. See, for example, Friedman et al. (2009);  
54 Efron and Hastie (2016); Dean and Ghemawat (2008); Zaharia et al. (2010); Abadi et al. (2016)  
55 and the references therein for more details.

56 In high-dimensional regression problems, we have a large number of predictors, and it is likely  
57 that only a subset of them have a relationship with the response and will be useful for prediction.  
58 Identifying such a subset is desirable for both scientific interests and the ability to predict outcomes  
59 in the future. The lasso (Tibshirani, 1996) is a widely used and effective method for simultaneous  
60 estimation and variable selection. Given a continuous response  $y \in \mathbb{R}^n$  and a model matrix  $X \in$   
61  $\mathbb{R}^{n \times p}$ , it solves the following regularized regression problem.

$$\hat{\beta}(\lambda) = \operatorname{argmin}_{\beta \in \mathbb{R}^p} \frac{1}{2n} \|y - X\beta\|_2^2 + \lambda \|\beta\|_1, \quad (1)$$

62 where  $\|x\|_q = (\sum_{i=1}^n |x_i|^q)^{1/q}$  is the vector  $\ell_q$  norm of  $x \in \mathbb{R}^n$  and  $\lambda \geq 0$  is the tuning parameter.  
63 The  $\ell_1$  penalty on  $\beta$  allows for selection as well as estimation. Normally there is an unpenalized  
64 intercept in the model, but for ease of presentation we leave it out, or we may assume that both  $X$   
65 and  $y$  have been centered with mean 0. One typically solves the entire lasso solution path over a grid  
66 of  $\lambda$  values  $\lambda_1 \geq \lambda_2 \cdots \geq \lambda_L$  and chooses the best  $\lambda$  by cross-validation or by predictive performance  
67 on an independent validation set. In R (R Core Team, 2017), several packages, such as **glmnet**  
68 (Friedman et al., 2010a) and **ncvreg** (Breheny and Huang, 2011), provide efficient procedures to  
69 obtain the solution path for the Gaussian model (1), and for other generalized linear models with the  
70 residual sum of squared replaced by the negative log-likelihood of the corresponding model. Among  
71 them, **glmnet**, equipped with highly optimized **Fortran** subroutines, is widely considered the fastest  
72 off-the-shelf lasso solver. It can, for example, fit a sequence of 100 logistic regression models on a  
73 sparse dataset with 54 million samples and 7 million predictors within only 2 hours (Hastie, 2015).

74 However, as the data become increasingly large, many existing methods and tools may not be  
75 able to serve the need, especially if the size exceeds the memory size. Most packages, including  
76 the ones mentioned above, assume that the data or at least its sparse representation can be fully  
77 loaded in memory and that the remaining memory is sufficient to hold other intermediate results.  
78 This becomes a real bottleneck for big datasets. For example, in our motivating application, the  
79 UK Biobank genotypes and phenotypes dataset (Bycroft et al., 2018) contains about 500,000 indi-  
80 viduals and more than 800,000 genotyped single nucleotide polymorphisms (SNPs) measurements  
81 per person. This provides unprecedented opportunities to explore more comprehensive genotypic  
82 relationships with phenotypes of interest. For polygenic traits such as height and body mass index  
83 (BMI), specific variants discovered by genome-wide association studies (GWAS) used to explain  
84 only a small proportion of the estimated heritability (Visscher et al., 2017), an upper bound of the  
85 proportion of phenotypic variance explained by the genetic components. While GWAS with larger  
86 sample size on the UK Biobank can be used to detect more SNPs and rare variants, their prediction  
87 performance is fairly limited by univariate models. It is very interesting to see if full-scale multiple  
88 regression methods such as the lasso or elastic-net can improve the prediction performance and  
89 simultaneously select relevant variants for the phenotypes. That being said, the computational  
90 challenges are two fold. First is the memory bound. Even though each bi-allelic SNP value can  
91 be represented by only two bits and the **PLINK** library (Chang et al., 2015) stores such SNP  
92 datasets in a binary compressed format, statistical packages such as **glmnet** and **ncvreg** require  
93 that the data be loaded in memory in a normal double-precision format. Given its sample size and  
94 dimension, the genotype matrix itself will take up around one terabyte of space, which may well  
95 exceed the size of the memory available and is infeasible for the packages. Second is the efficiency  
96 bound. For a larger-than-RAM dataset, it has to sit on the disk and we may only read part of it  
97 into the memory. In such scenario, the overall efficiency of the algorithm is not only determined  
98 by the number of basic arithmetic operations but also the disk I/O — data transfer between the  
99 memory and the disk — an operation several magnitudes slower than in-memory operations.

100 In this paper, we propose an efficient and scalable meta algorithm for the lasso called Batch  
101 Screening Iterative Lasso (BASIL) that is applicable to larger-than-RAM datasets and designed

102 to tackle the memory and efficiency bound. It computes the entire lasso path and can easily  
103 build on any existing package to make it a scalable solution. As the name suggests, it is done in  
104 an iterative fashion on an adaptively screened subset of variables. At each iteration, we exploit an  
105 efficient, parallelizable screening operation to significantly reduce the problem to one of manageable  
106 size, solve the resulting smaller lasso problem, and then reconstruct and validate a full solution  
107 through another efficient, parallelizable step. In other words, the iterations have a screen-solve-  
108 check substructure. That being said, it is the goal and also the guarantee of the BASIL algorithm  
109 that the final solution exactly solves the full lasso problem (1) rather than any approximation, even  
110 if the intermediate steps work repeatedly on subsets of variables.

111 The screen-solve-check substructure is inspired by Tibshirani et al. (2012) and especially the  
112 proposed strong rules. The strong rules state: assume  $\hat{\beta}(\lambda_{k-1})$  is the lasso solution in (1) at  $\lambda_{k-1}$ ,  
113 then the  $j$ th predictor is discarded at  $\lambda_k$  if

$$|x_j^\top (y - X\hat{\beta}(\lambda_{k-1}))| < \lambda_k - (\lambda_{k-1} - \lambda_k). \quad (2)$$

114 The key idea is that the inner product above is almost “non-expansive” in  $\lambda$  and that the lasso  
115 solution is characterized equivalently by the Karush-Kuhn-Tucker (KKT) condition (Boyd and  
116 Vandenberghe, 2004). For the lasso, the KKT condition states that  $\hat{\beta} \in \mathbb{R}^p$  is a solution to (1) if  
117 for all  $1 \leq j \leq p$ ,

$$\frac{1}{n} \cdot x_j^\top (y - X\hat{\beta}) \begin{cases} = \lambda \cdot \text{sign}(\hat{\beta}_j), & \text{if } \hat{\beta}_j \neq 0, \\ \leq \lambda, & \text{if } \hat{\beta}_j = 0. \end{cases} \quad (3)$$

118 The KKT condition suggests that the variables discarded based on the strong rules would have  
119 coefficient 0 at the next  $\lambda_k$ . The checking step comes into play because this is not a guarantee. The  
120 strong rules can fail, though failures occur rarely when  $p > n$ . In any case, the KKT condition will  
121 be checked to see if the coefficients of the left-out variables are indeed 0 at  $\lambda_k$ . If the check fails,  
122 we add in the violated variables and repeat the process. Otherwise, we successfully reconstruct a  
123 full solution and move to the next  $\lambda$ . This is the iterative algorithm proposed by these authors and  
124 has been implemented efficiently into the **glmnet** package.

125 The BASIL algorithm proceeds in a similar way but is designed to optimize for datasets that  
126 are too big to fit into the memory. Considering the fact that screening and KKT check need to scan  
127 through the entire data and are thus costly in the disk Input/Output (I/O) operations, we attempt  
128 to do batch screening and solve *a series of* models (at different  $\lambda$  values) in each iteration, where a  
129 single sweep over the full data would suffice. Followed by a checking step, we can obtain the lasso  
130 solution for multiple  $\lambda$ 's in one iteration. This can effectively reduce the total number of iterations  
131 needed to compute the full solution path and thus reduce the expensive disk read operations that  
132 often cause significant delay in the computation. The process is illustrated in Figure 1 and will be  
133 detailed in the next section.

## 134 2 Results

135 **Overview of the BASIL algorithm** For convenience, we first introduce some notation. Let  
136  $\Omega = \{1, 2, \dots, p\}$  be the universe of variable indices. For  $1 \leq \ell \leq L$ , let  $\hat{\beta}(\lambda_\ell)$  be the lasso solution  
137 at  $\lambda = \lambda_\ell$ , and  $\mathcal{A}(\lambda_\ell) = \{1 \leq j \leq p : \hat{\beta}_j(\lambda_\ell) \neq 0\}$  be the active set. When  $X$  is a matrix, we use  $X_{\mathcal{S}}$   
138 to represent the submatrix including only columns indexed by  $\mathcal{S}$ . Similarly when  $\beta$  is a vector,  $\beta_{\mathcal{S}}$   
139 represents the subvector including only elements indexed by  $\mathcal{S}$ . Given any two vectors  $a, b \in \mathbb{R}^n$ ,  
140 the dot product or inner product can be written as  $a^\top b = \langle a, b \rangle = \sum_{i=1}^n a_i b_i$ . Throughout the  
141 paper, we use predictors, features, variables and variants interchangeably. We use the strong set to  
142 refer to the screened subset of variables on which the lasso fit is computed at each iteration, and  
143 the active set to refer to the subset of variables with nonzero lasso coefficients.

144 Remember that our goal is to compute the exact lasso solution (1) for larger-than-RAM datasets  
145 over a grid of regularization parameters  $\lambda_1 > \lambda_2 > \dots > \lambda_L \geq 0$ . We describe the procedure for the  
146 Gaussian family in this section and discuss extension to general problems in the next. A common  
147 choice is  $L = 100$  and  $\lambda_1 = \max_{1 \leq j \leq p} |x_j^\top r^{(0)}|/n$ , the largest  $\lambda$  at which the estimated coefficients  
148 start to deviate from zero. Here  $r^{(0)} = y$  if we do not include an intercept term and  $r^{(0)} = y - \bar{y}$   
149 if we do. In general,  $r^{(0)}$  is the residual of regressing  $y$  on the unpenalized variables, if any. The  
150 other  $\lambda$ 's can be determined, for example, by an equally spaced array on the log scale. The solution

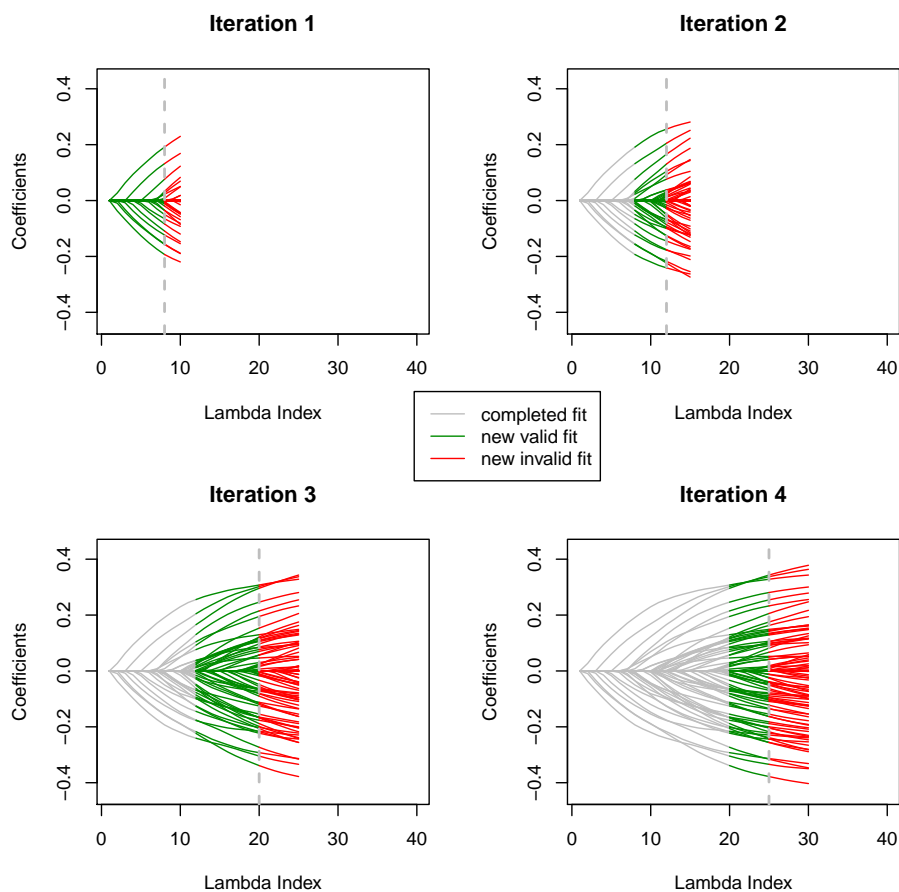


**Figure 1:** The lasso coefficient profile that shows the progression of the BASIL algorithm. The previously finished part of the path is colored grey, the newly completed and verified is in green, and the part that is newly computed but failed the verification is colored red.

151 path is found iteratively with a screening-solving-checking substructure similar to the one proposed  
 152 in Tibshirani et al. (2012). Designed for large-scale and ultrahigh-dimensional data, the BASIL  
 153 algorithm can be viewed as a batch version of the strong rules. At each iteration we attempt to  
 154 find valid lasso solution for *multiple*  $\lambda$  values on the path and thus reduce the burden of disk reads  
 155 of the big dataset. Specifically, as summarized in Algorithm 1, we start with an empty strong set  
 156  $\mathcal{S}^{(0)} = \emptyset$  and active set  $\mathcal{A}^{(0)} = \emptyset$ . Each of the following iterations consists of three steps: screening,  
 157 fitting and checking.

---

**Algorithm 1** BASIL for the Gaussian Model

---

- 1: **Initialization:** active set  $\mathcal{A}^{(0)} = \emptyset$ , initial residual  $r^{(0)}$  (with respect to the intercept or other unpenalized variables) at  $\lambda_1 = \lambda_{\max}$ , a short list of initial parameters  $\Lambda^{(0)} = \{\lambda_1, \dots, \lambda_{L^{(0)}}\}$ .
- 2: **for**  $k = 0$  **to**  $K$  **do**
- 3: **Screening:** for each  $1 \leq j \leq p$ , compute inner product with current residual  $c_j^{(k)} = \langle x_j, r^{(k)} \rangle$ . Construct the strong set

$$\mathcal{S}^{(k)} = \mathcal{A}^{(k)} \cup \mathcal{E}_M^{(k)},$$

where  $\mathcal{E}_M^{(k)}$  is the set of  $M$  variables in  $\Omega \setminus \mathcal{A}^{(k)}$  with largest  $|c^{(k)}|$ .

- 4: **Fitting:** for all  $\lambda \in \Lambda^{(k)}$ , solve the lasso only on the strong set  $\mathcal{S}^{(k)}$ , and find the coefficients  $\hat{\beta}^{(k)}(\lambda)$  and the residuals  $r^{(k)}(\lambda)$ .
- 5: **Checking:** search for the smallest  $\lambda$  such that the KKT conditions are satisfied, i.e.,

$$\bar{\lambda}^{(k)} = \min \left\{ \lambda \in \Lambda^{(k)} : \max_{j \in \Omega \setminus \mathcal{S}^{(k)}} (1/n) |x_j^\top r^{(k)}(\lambda)| < \lambda \right\}.$$

For empty set, we define  $\bar{\lambda}^{(k)}$  to be the immediate previous  $\lambda$  to  $\Lambda^{(k)}$  but increment  $M$  by  $\Delta M$ . Let the current active set  $\mathcal{A}^{(k+1)}$  and residuals  $r^{(k+1)}$  defined by the solution at  $\bar{\lambda}^{(k)}$ . Define the next parameter list  $\Lambda^{(k+1)} = \{\lambda \in \Lambda^{(k)} : \lambda < \bar{\lambda}^{(k)}\}$ . Extend this list if it consists of too few elements. For  $\lambda \in \Lambda^{(k)} \setminus \Lambda^{(k+1)}$ , we obtain exact lasso solutions for the full problem:

$$\hat{\beta}_{\mathcal{S}^{(k)}}(\lambda) = \hat{\beta}^{(k)}(\lambda), \quad \hat{\beta}_{\Omega \setminus \mathcal{S}^{(k)}}(\lambda) = 0.$$

---

6: **end for**

---

158 In the screening step, an updated strong set is found as the candidate for the subsequent fitting.  
 159 Suppose that so far (valid) lasso solutions have been found for  $\lambda_1, \dots, \lambda_\ell$  but not for  $\lambda_{\ell+1}$ . The new  
 160 set will be based on the lasso solution at  $\lambda_\ell$ . In particular, we will select the top  $M$  variables with  
 161 largest absolute inner products  $|\langle x_j, y - X\hat{\beta}(\lambda_\ell) \rangle|$ . They are the variables that are most likely to be  
 162 active in the lasso model for the next  $\lambda$  values. In addition, we include the ever-active variables at  
 163  $\lambda_1, \dots, \lambda_\ell$  because they have been “important” variables and might continue to be important at a  
 164 later stage.

165 In the fitting step, the lasso is fit on the updated strong set for the next  $\lambda$  values  $\lambda_{\ell+1}, \dots, \lambda_{\ell'}$ .  
 166 Here  $\ell'$  is often smaller than  $L$  because we do not have to solve for all of the remaining  $\lambda$  values on  
 167 this strong set. The full lasso solutions at much smaller  $\lambda$ 's are very likely to have active variables  
 168 outside of the current strong set. In other words even if we were to compute solutions for those  
 169 very small  $\lambda$  values on the current strong set, they would probably fail the KKT test. These  $\lambda$ 's



170 are left to later iterations when the strong set is expanded.

171 In the checking step, we check if the newly obtained solutions on the strong set can be valid  
172 part of the full solutions by evaluating the KKT condition. Given a solution  $\hat{\beta}_S \in \mathbb{R}^{|S|}$  to the  
173 sub-problem at  $\lambda$ , if we can verify for every left-out variable  $j$  that  $(1/n)|\langle x_j, y - X_S \hat{\beta}_S \rangle| < \lambda$ , we  
174 can then safely set their coefficients to 0. The full lasso solution  $\hat{\beta}(\lambda) \in \mathbb{R}^p$  is then assembled by  
175 letting  $\hat{\beta}_S(\lambda) = \hat{\beta}_S$  and  $\hat{\beta}_{\Omega \setminus S}(\lambda) = 0$ . We look for the  $\lambda$  value prior to the one that causes the first  
176 failure down the  $\lambda$  sequence and use its residual as the basis for the next screening. Nevertheless,  
177 there is still chance that none of the solutions on the current strong set passes the KKT check  
178 for the  $\lambda$  subsequence considered in this iterations. That suggests the number of previously added  
179 variables in the current iteration was not sufficient. In this case, we are unable to move forward  
180 along the  $\lambda$  sequence, but will fall back to the  $\lambda$  value where the strong set was last updated and  
181 include  $\Delta M$  more variables based on the sorted absolute inner product.

182 The three steps above can be applied repeatedly to roll out the complete lasso solution path  
183 for the original problem. However, if our goal is choosing the best model along the path, we can  
184 stop fitting once an optimal model is found evidenced by the performance on a validation set. At a  
185 high level, we run the iterative procedure on the training data, monitor the error on the validation  
186 set, and stop when the model starts to overfit, or in other words, when the validation error shows  
187 a clear upward trend.

188 **Extension to general problems** It is straightforward to extend the algorithm from the Gaussian  
189 case to more general problems. In fact, the only changes we need to make are the screening step  
190 and the strong set update step. Wherever the strong rules can be applied, we have a corresponding  
191 version of the iterative algorithm. In Tibshirani et al. (2012), the general problem is

$$\hat{\beta}(\lambda) = \operatorname{argmin}_{\beta \in \mathbb{R}^p} f(\beta) + \lambda \sum_{j=1}^r c_j \|\beta_j\|_{p_j}, \quad (4)$$

192 where  $f$  is a convex differentiable function, and for all  $1 \leq j \leq r$ ,  $c_j \geq 0, p_j \geq 1$ , and  $\beta_j$  can be a  
193 scalar or vector whose  $\ell_{p_j}$ -norm is represented by  $\|\beta_j\|_{p_j}$ . The general strong rule discards predictor

194  $j$  if

$$\|\nabla_j f(\hat{\beta}(\lambda_{k-1}))\|_{q_j} < c_j(2\lambda_k - \lambda_{k-1}), \quad (5)$$

195 where  $1/p_j + 1/q_j = 1$ . Hence, our algorithm can adapt and screen by choosing variables with  
 196 large values of  $\|\nabla_j f(\hat{\beta}(\lambda_{k-1}))\|_{q_j}$  that are not in the current active set. We expand in more detail  
 197 two important applications of the general rule: logistic regression and Cox's proportional hazards  
 198 model in survival analysis.

**Logistic regression** In the lasso penalized logistic regression (Friedman et al., 2010b) where the observed outcome  $y \in \{0, 1\}^n$ , the convex differential function in (4) is

$$f(\beta) = -\frac{1}{n} \sum_{i=1}^n (y_i \log p_i + (1 - y_i) \log(1 - p_i)).$$

where  $p_i = 1/(1 + \exp(-x_i^\top \beta))$  for all  $1 \leq i \leq n$ . The rule in (5) is reduced to

$$|x_j^\top (y - \hat{p}(\lambda_{k-1}))| < \lambda_k - (\lambda_{k-1} - \lambda_k),$$

199 where  $\hat{p}(\lambda_{k-1})$  is the predicted probabilities at  $\lambda = \lambda_{k-1}$ . Similar to the Gaussian case, we can still  
 200 fit relaxed lasso and allow adjustment covariates in the model to adjust for confounding effect.

**Cox's proportional hazards model** In the usual survival analysis framework, for each sample, in addition to the predictors  $x_i \in \mathbb{R}^p$  and the observed time  $y_i$ , there is an associated right-censoring indicator  $\delta_i \in \{0, 1\}$  such that  $\delta_i = 0$  if failure and  $\delta_i = 1$  if right-censored. Let  $t_1 < t_2 < \dots < t_m$  be the increasing list of unique failure times, and  $j(i)$  denote the index of the observation failing at time  $t_i$ . The Cox's proportional hazards model (Cox, 1972) assumes the hazard for the  $i$ th individual as  $h_i(t) = h_0(t) \exp(x_i^\top \beta)$  where  $h_0(t)$  is a shared baseline hazard at time  $t$ . We can let  $f(\beta)$  be the negative log partial likelihood in (4) and screen based on its gradient at the most recent

lasso solution as suggested in (5). In particular,

$$f(\beta) = -\frac{1}{m} \sum_{i=1}^m \left( x_{j(i)}^\top \beta - \log \left( \sum_{j \in R_i} \exp(x_j^\top \beta) \right) \right),$$

201 where  $R_i$  is the set of indices  $j$  with  $y_j \geq t_i$  (those at risk at time  $t_i$ ). We can derive the associated  
202 rule based on (5) and thus the survival BASIL algorithm. Further discussion and comprehensive  
203 experiments are included in a follow-up paper (Li et al., 2020).

204 **Extension to the elastic net** Our discussion so far focuses solely on the lasso penalty, which  
205 aims to achieve a rather sparse set of linear coefficients. In spite of good performance in many high-  
206 dimensional settings, it has limitations. For example, when there is a group of highly correlated  
207 variables, the lasso will often pick out one of them and ignore the others. This poses some hardness  
208 in interpretation. Also, under high-correlation structure like that, it has been empirically observed  
209 that when the predictors are highly correlated, the ridge can often outperform the lasso (Tibshirani,  
210 1996).

211 The elastic net, proposed in Zou and Hastie (2005), extends the lasso and tries to find a sweet  
212 spot between the lasso and the ridge penalty. It can capture the grouping effect of highly correlated  
213 variables and sometimes perform better than both methods especially when the number of variables  
214 is much larger than the number of samples. In particular, instead of imposing the  $\ell_1$  penalty, the  
215 elastic net solves the following regularized regression problem.

$$\hat{\beta}(\lambda) = \underset{\beta \in \mathbb{R}^p}{\operatorname{argmin}} f(\beta) + \lambda(\alpha \|\beta\|_1 + (1 - \alpha) \|\beta\|_2^2 / 2), \quad (6)$$

216 where the mixing parameter  $\alpha \in [0, 1]$  determines the proportion of lasso and ridge in the penalty  
217 term.

218 It is straightforward to adapt the BASIL procedure to the elastic net. It follows from the gradient  
219 motivation of the strong rules and KKT condition of convex optimization. We take the Gaussian  
220 family as an example. The others are similar. In the screening step, it is easy to derive that we can

221 still rank *among the currently inactive variables* on their absolute inner product with the residual  
222  $|x_j^\top (y - X\hat{\beta}(\lambda_{k-1}))|$  to determine the next candidate set. In the checking step, to verify that all the  
223 left-out variables indeed have zero coefficients, we need to make sure that  $(1/n)|x_j^\top (y - X\hat{\beta}(\lambda_{k-1}))| \leq$   
224  $\lambda\alpha$  holds for all such variables. It turns out that in our UK Biobank applications, the elastic-net  
225 results (after selection of  $\alpha$  and  $\lambda$  on the validation set) do not differ significantly from the lasso  
226 results, which will be immediately seen in the next section.

227 **UK Biobank analysis** We describe a real-data application on the UK Biobank that in fact  
228 motivates our development of the BASIL algorithm.

229 The UK Biobank (Bycroft et al., 2018) is a very large, prospective population-based cohort  
230 study with individuals collected from multiple sites across the United Kingdom. It contains exten-  
231 sive genotypic and phenotypic detail such as genomewide genotyping, questionnaires and physical  
232 measures for a wide range of health-related outcomes for over 500,000 participants, who were aged  
233 40-69 years when recruited in 2006-2010. In this study, we are interested in the relationship between  
234 an individual's genotype and his/her phenotypic outcome. While GWAS focus on identifying SNPs  
235 that may be marginally associated with the outcome using univariate tests, we would like to find  
236 relevant SNPs in a multivariate prediction model using the lasso. A recent study (Lello et al., 2018)  
237 fits the lasso on a subset of the variables after one-shot univariate  $p$ -value screening and suggests  
238 improvement in explaining the variation in the phenotypes. However, the left-out variants with  
239 relatively weak marginal association may still provide additional predictive power in a multiple  
240 regression environment. The BASIL algorithm enables us to fit the lasso model at full scale and  
241 gives further improvement in the explained variance over the alternative models considered.

242 We focused on 337,199 White British unrelated individuals out of the full set of over 500,000 from  
243 the UK Biobank dataset (Bycroft et al., 2018) that satisfy the same set of population stratification  
244 criteria as in DeBoever et al. (2018). The dataset is partitioned randomly into training, validation  
245 and test subsets. Each individual has up to 805,426 measured variants, and each variant is encoded  
246 by one of the four levels where 0 corresponds to homozygous major alleles, 1 to heterozygous alleles,  
247 2 to homozygous minor alleles and NA to a missing genotype. In addition, we have available

248 covariates such as age, sex, and forty pre-computed principal components of the SNP matrix.

To evaluate the predictive performance for quantitative response, we use a common measure R-squared ( $R^2$ ). Given a linear estimator  $\hat{\beta}$  and data  $(y, X)$ , it is defined as

$$R^2 = 1 - \frac{\|y - X\hat{\beta}\|_2^2}{\|y - \bar{y}\|_2^2}.$$

249 We evaluate this criteria for all the training, validation and test sets. For a dichotomous response,  
250 misclassification error could be used but it would depend on the calibration. Instead the receiver  
251 operating characteristic (ROC) curve provides more information and illustrates the tradeoff between  
252 true positive and false positive rates under different thresholds. The AUC computes the area under  
253 the ROC curve — a larger value indicates a generally better classifier. Therefore, we will evaluate  
254 AUCs on the training, validation and test sets for dichotomous responses.

255 We compare the performance of the lasso with related methods to have a sense of the contribution  
256 of different components. Starting from the baseline, we fit a linear model that includes only age  
257 and sex (Model 1 in the tables below), and then one that includes additionally the top 10 principal  
258 components (Model 2). These are the adjustment covariates used in our main lasso fitting and we  
259 use these two models to highlight the contribution of the SNP information over and above that of  
260 age, sex and the top 10 PCs. In addition, the strongest univariate model is also evaluated (Model  
261 3). This includes the 12 adjustment covariates together with the single SNP that is most correlated  
262 with the outcome after adjustment.

263 Toward multivariate models, we first compare with a univariate method that has some multi-  
264 variate flavor (Models 4 and 5). We select a subset of the  $K$  most marginally significant variants  
265 (after adjusting for the covariates), and construct a new variable by linearly combining these vari-  
266 ants using their univariate coefficients. An OLS is then fit on the new variable together with the  
267 adjustment variables. It is similar to a one-step partial least squares (Wold, 1975) with  $p$ -value  
268 based truncation. We take  $K = 10,000$  and  $100,000$  in the experiments. We further compare with  
269 a hierarchical sequence of multivariate models where each is fit on a subset of the most significant  
270 SNPs. In particular, the  $\ell$ -th model selects  $\ell \times 1000$  SNPs with the smallest univariate  $p$ -values, and

271 a multivariate linear or logistic regression is fit on those variants jointly. The sequence of models  
272 are evaluated on the validation set, and the one with the smallest validation error is chosen. We  
273 call this method Sequential LR or SeqLR (Model 6) for convenience in the rest of the paper. As  
274 a byproduct of the lasso, the relaxed lasso (Meinshausen, 2007) fits a debiased model by refitting  
275 an OLS on the variables selected by the lasso. This can potentially recover some of the bias in-  
276 troduced by lasso shrinkage. For the elastic-net, we fit separate solution paths with varying  $\lambda$ 's at  
277  $\alpha = 0.1, 0.5, 0.9$ , and evaluate their performance ( $R^2$  or AUC) on the validation set. The best pair  
278 of hyperparameters  $(\alpha, \lambda)$  is selected and the corresponding test performance is reported.

279 In addition, we make comparison with two other bayesian methods PRS-CS (Ge et al., 2019)  
280 and SBayesR (Lloyd-Jones et al., 2019). For PRS-CS, we first characterized the GWAS summary  
281 statistics using the combined set of training and validation set ( $n = 269,927$ ) with age, sex, and  
282 the top 10 PCs as covariates using PLINK v2.00a3LM (9 Apr 2020) (Chang et al., 2015). Using  
283 the LD reference dataset precomputed for the European Ancestry using the 1000 genome samples  
284 (<https://github.com/getian107/PRScs>), we applied PRS-CS with the default option. We took  
285 the posterior effect size estimates and computed the polygenic risk scores using PLINK2's `--score`  
286 subcommand (Chang et al., 2015). For SBayesR, we computed the sparse LD matrix using the com-  
287 bined set of training and validation set individuals ( $n = 269,927$ ) using the `--make-sparse-ldm`  
288 subcommand implemented in GCTB version 2.0.1 (Zeng et al., 2018). Using the GWAS sum-  
289 mary statistics computed on the set of individuals and following the GCTB's recommendations,  
290 we applied SBayesR with the following options: `gctb --sbayes R--ldm [the LD matrix] --pi`  
291 `0.95,0.02,0.02,0.01 --gamma 0.0,0.01,0.1,1 --chain-length 10000 --burn-in 2000`  
292 `--exclude-mhc --gwas-summary [the GWAS summary statistics]`. We report the model per-  
293 formance on the test set.

294 There are thousands of measured phenotypes in the dataset. For demonstration purpose, we  
295 analyze four phenotypes that are known to be highly or moderately heritable and polygenic. For  
296 these complex traits, univariate studies may not find SNPs with smaller effects, but the lasso model  
297 may include them and predict the phenotype better. We look at two quantitative traits: standing  
298 height and body mass index (BMI) (Tanigawa et al., 2019), and two qualitative traits: asthma and

299 high cholesterol (HC) (DeBoever et al., 2018).

300 We first summarize the test performance of different methods on the four phenotypes in Figure 2.  
 301 The lasso and elastic net show significant improvement in test  $R^2$  and AUC over the other competing  
 302 methods. Details of the model for height are given in the next section and for the other phenotypes  
 303 (BMI, asthma and high cholesterol) in Appendix A. A comparison of the univariate  $p$ -values and  
 304 the lasso coefficients for all these traits is shown in the form of Manhattan plots in the Appendix  
 305 B (Supplementary Figure 14, 15).

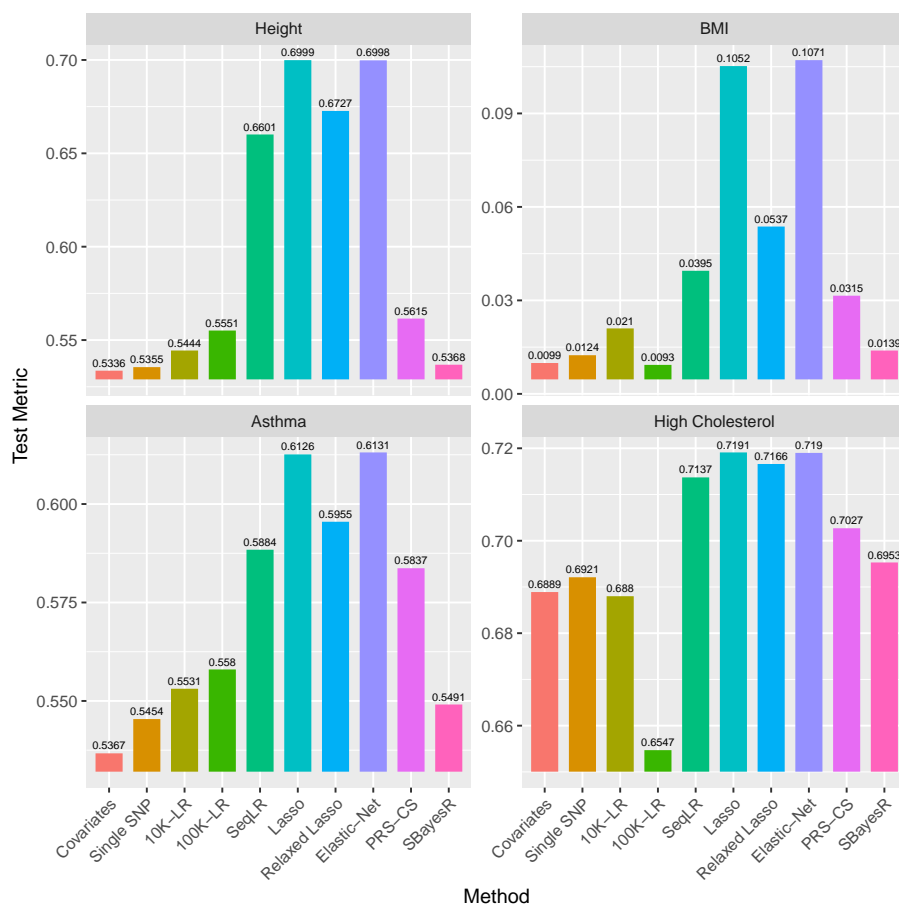


**Figure 2:** Comparison of different methods on the test set.  $R^2$  are evaluated for continuous phenotypes height and BMI, and AUC evaluated for binary phenotypes asthma and high cholesterol.

306 Height is a polygenic and heritable trait that has been studied for a long time. It has been used

307 as a model for other quantitative traits, since it is easy to measure reliably. From twin and sibling  
 308 studies, the narrow sense heritability is estimated to be 70-80% (Silventoinen et al., 2003; Visscher  
 309 et al., 2006, 2010). Recent estimates controlling for shared environmental factors present in twin  
 310 studies calculate heritability at 0.69 (Zaitlen et al., 2013; Hemani et al., 2013). A linear based  
 311 model with common SNPs explains 45% of the variance (Yang et al., 2010) and a model including  
 312 imputed variants explains 56% of the variance, almost matching the estimated heritability (Yang  
 313 et al., 2015). So far, GWAS studies have discovered 697 associated variants that explain one fifth  
 314 of the heritability (Lango Allen et al., 2010; Wood et al., 2014). Recently, a large sample study  
 315 was able to identify more variants with low frequencies that are associated with height (Marouli  
 316 et al., 2017). Using lasso with the larger UK Biobank dataset allows both a better estimate of the  
 317 proportion of variance that can be explained by genomic predictors and simultaneous selection of  
 318 SNPs that may be associated. The results are summarized in Table 1. The associated  $R^2$  curves for  
 319 the lasso and the relaxed lasso are shown in Figure 3. The residuals of the optimal lasso prediction  
 320 are plotted in Figure 4.

Model	Form	$R^2_{\text{train}}$	$R^2_{\text{val}}$	$R^2_{\text{test}}$	Size
(1)	Age + Sex	0.5300	0.5260	0.5288	2
(2)	Age + Sex + 10 PCs	0.5344	0.5304	0.5336	12
(3)	Strong Single SNP	0.5364	0.5323	0.5355	13
(4)	10K Combined	0.5482	0.5408	0.5444	10,012
(5)	100K Combined	0.5833	0.5515	0.5551	100,012
(6)	Sequential LR	0.7416	0.6596	0.6601	17,012
(7)	Lasso	0.8304	0.6992	<b>0.6999</b>	47,673
(8)	Relaxed Lasso	0.7789	0.6718	0.6727	13,395
(9)	Elastic Net	0.8282	0.6991	0.6998	48,256
(10)	PRS-CS	0.5692	—	0.5615	148,052
(11)	SBayesR	0.5397	—	0.5368	667,045

**Table 1:**  $R^2$  values for height. For sequential LR, lasso and relaxed lasso, the chosen model is based on maximum  $R^2$  on the validation set. Model (3) to (8) each includes Model (2) plus their own specification as stated in the Form column. The validation results for PRS-CS and SBayesR are not available because we used a combined training and validation set for training.

321 A large number (47,673) of SNPs need to be selected in order to achieve the optimal  $R^2_{\text{test}} =$   
 322 0.6999 for the lasso and similarly for the elastic-net. Comparatively, the relaxed lasso sacrifices  
 323 some predictive performance by including a much smaller subset of variables (13,395). Past the



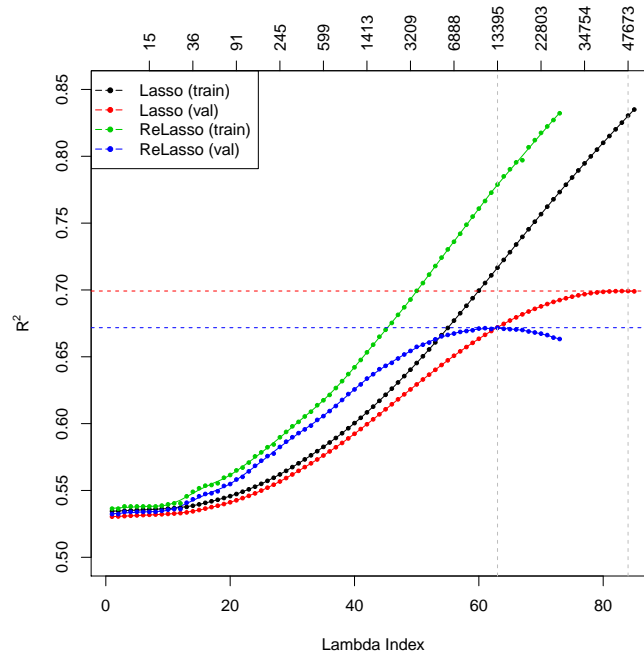


**Figure 3:**  $R^2$  plot for height. The top axis shows the number of active variables in the model.

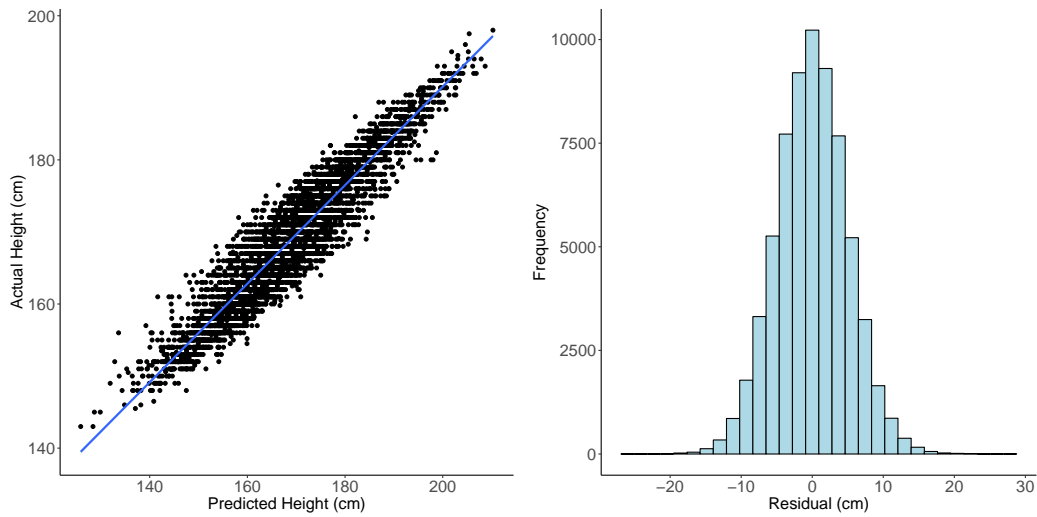


**Figure 4:** Left: actual height versus predicted height on 5000 random samples from the test set. The correlation between actual height and predicted height is 0.9416. Right: histogram of the lasso residuals for height. Standard deviation of the residual is 5.05 (cm).

Method	$R^2_{\text{val}}$	$R^2_{\text{test}}$	$h^2_{\text{test}}$	$\text{Cor}_{\text{test}}$	$\text{Cor}_{\text{test}} - \{\text{age, sex}\}$
Lasso	69.92%	69.99%	35.66%	0.8366	0.4079
Prescreened lasso	69.40%	69.56%	34.73%	0.8340	0.4025

**Table 2:** Comparison of prediction results on height with the model trained following the same procedure as ours except for an additional prescreening step as done in Lello et al. (2018). In addition to  $R^2$ , proportion of residual variance explained (denoted by  $h^2_{\text{test}}$ ) and correlation between the fitted values and actual values are computed. We also compute an adjusted correlation between the residual after regressing age and sex out from the prediction and the residual after regressing age and sex out from the true response, both on the test set.

324 optimal point, the additional variance introduced by refitting such large models may be larger than  
325 the reduction in bias. The large models confirm the extreme polygenicity of standing height.

326 In comparison to the other models, the lasso performs significantly better in terms of  $R^2_{\text{test}}$   
327 than all univariate methods, and outperforms multivariate methods based on univariate  $p$ -value  
328 ordering. That demonstrates the value of simultaneous variable selection and estimation from a  
329 multivariate perspective, and enables us to predict height to within 10 cm about 95% of the time  
330 based only on SNP information (together with age and sex). We also notice that the sequential  
331 linear regression approach does a good job, whose performance gets close to that of the relaxed  
332 lasso. It is straightforward and easy to implement using existing softwares such as **PLINK** (Chang  
333 et al., 2015).

334 Recently Lello et al. (2018) apply a lasso based method to predict height and other phenotypes  
335 on the UK Biobank. Instead of fitting on all QC-satisfied SNPs (as stated in Section 4), they  
336 pre-screen 50K or 100K most significant SNPs in terms of  $p$ -value and apply lasso on that set only.  
337 In addition, although both datasets come from the same UK Biobank, the subset of individuals  
338 they used is larger than ours. While we restrict the analysis to the unrelated individuals who have  
339 self-reported white British ancestry, they look at Europeans including British, Irish and Any Other  
340 White. For a fair comparison, we follow their procedure (pre-screening 100K SNPs) but run on  
341 our subset of the dataset. The results are shown in Table 2. We see that the improvement of the  
342 full lasso over the prescreened lasso is almost 0.5% in test  $R^2$ , and 1% relative to the proportion of  
343 residual variance explained after covariate adjustment.

344 Further, we compare the full lasso coefficients and the univariate  $p$ -values from GWAS in Fig-

ure 5. The vertical grey dotted line indicates the top 100K cutoff in terms of  $p$ -value. We see

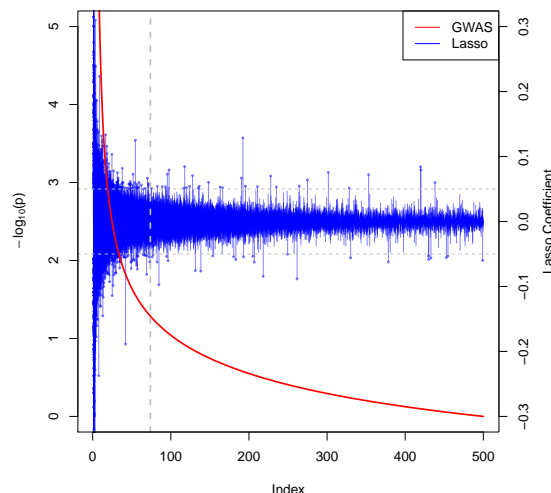


**Figure 5:** Comparison of the lasso coefficients and univariate  $p$ -values for height. The index on the horizontal axis represents the SNPs sorted by their univariate  $p$ -values. The red curve associated with the left vertical axis shows the  $-\log_{10}$  of the univariate  $p$ -values. The blue bars associated with the right vertical axis show the corresponding lasso coefficients for each (sorted) SNP. The horizontal dotted lines in gray identifies lasso coefficients of  $\pm 0.05$ . The vertical one represents the 100K cutoff used in Lello et al. (2018).

345

346 although a general decreasing trend appears in the magnitude of the lasso coefficients with respect  
347 to increasing  $p$ -values (decreasing  $-\log_{10}(p)$ ), there are a number of spikes even in the large  $p$ -value  
348 region which is considered marginally insignificant. This shows that variants beyond the strongest  
349 univariate ones contribute to prediction.

### 350 3 Discussion

351 In this paper, we propose a novel batch screening iterative lasso (BASIL) algorithm to fit the full  
352 lasso solution path for very large and high-dimensional datasets. It can be used, among the others,  
353 for Gaussian linear model, logistic regression and Cox regression, and can be easily extended to fit  
354 the elastic-net with mixed  $\ell_1/\ell_2$  penalty. It enjoys the advantages of high efficiency, flexibility and  
355 easy implementation. For SNP data as in our applications, we develop an R package **snpnet** that

356 incorporates SNP-specific optimizations and are able to process datasets of wide interest from the  
357 UK Biobank.

358 In our algorithm, the choice of  $M$  is important for the practical performance. It trades off  
359 between the number of iterations and the computation per iteration. With a small  $M$  or small  
360 update of the strong set, it is very likely that we are unable to proceed fast along the  $\lambda$  sequence in  
361 each iteration. Although the design of the BASIL algorithm guarantees that for any  $M, \Delta M > 0$ ,  
362 we are able to obtain the full solution path after sufficient iterations, many iterations will be needed  
363 if  $M$  is chosen too small, and the disk I/O cost will be dominant. In contrast, a large  $M$  will incur  
364 more memory burden and more expensive lasso computation, but with the hope to find more valid  
365 lasso solutions in one iteration, save the number of iterations and the disk I/O. It is hard to identify  
366 the optimal  $M$  a priori. It depends on the computing architecture, the size of the problem, the  
367 nature of the phenotype, etc. For this reason, we tend to leave it as a subjective parameter to  
368 the user's choice. However in the meantime, we do plan to provide a more systematic option to  
369 determine  $M$ , which leverages the strong rules again. Recall that in the simple setting with no  
370 intercept and no covariates, the initial strong set is constructed by  $|x_j^\top y| \leq 2\lambda - \lambda_{\max}$ . Since the  
371 strong rules rarely make mistakes and are fairly effective in discarding inactive variables, we can  
372 guide the choice of batch size  $M$  by the number of  $\lambda$  values we want to cover in the first iteration.  
373 For example, one may want the strong set to be large enough to solve for the first 10  $\lambda$ 's in the  
374 first iteration. We can then let  $M = |\{1 \leq j \leq p : |x_j^\top y| > 2\lambda_{10} - \lambda_{\max}\}|$ . Despite being adaptive  
375 to the data in some sense, this approach is by no means computationally optimal. It is more based  
376 on heuristics that the iteration should make reasonable progress along the path.

377 Our numerical studies demonstrate that the iterative procedure effectively reduces a big- $n$ -big-  
378  $p$  lasso problem into one that is manageable by in-memory computation. In each iteration, we  
379 are able to use parallel computing when applying screening rules to filter out a large number of  
380 variables. After screening, we are left with only a small subset of data on which we are able to  
381 conduct intensive computation like cyclical coordinate descent all in memory. For the subproblem,  
382 we can use existing fast procedures for small or moderate-size lasso problems. Thus, our method  
383 allows easy reuse of previous software with lightweight development effort.

384 When a large number of variables is needed in the optimal predictive model, it may still require  
385 either large memory or long computation time to solve the smaller subproblem. In that case, we  
386 may consider more scalable and parallelizable methods like proximal gradient descent (Parikh and  
387 Boyd, 2014) or dual averaging (Xiao, 2010; Duchi et al., 2012). One may think why don't we  
388 directly use these methods for the original full problem? First, the ultra high dimension makes  
389 the evaluation of gradients, even on mini-batch very expensive. Second, it can take a lot more  
390 steps for such first-order methods to converge to a good objective value. Moreover, the speed of  
391 convergence depends on the choice of other parameters such as step size and additional constants  
392 in dual averaging. For those reasons, we still prefer the tuning-free and fast coordinate descent  
393 methods when the subproblem is manageable.

394 The lasso has nice variable selection and prediction properties if the linear model assumption  
395 together with some additional assumptions such as the restricted eigenvalue condition (Bickel et al.,  
396 2009) or the irrepresentable condition (Zhao and Yu, 2006) holds. In practice, such assumptions do  
397 not always hold and are often hard to verify. In our UK Biobank application, we don't attempt to  
398 verify the exact conditions, and the selected model can be subject to false positives. However, we  
399 demonstrate relevance of the selection via empirical consistency with the GWAS results. We have  
400 seen superior prediction performance by the lasso as a regularized regression method compared to  
401 other methods. More importantly, by leveraging the sparsity property of the lasso, we are able to  
402 manage the ultrahigh-dimensional problem and obtain a computationally efficient solution.

403 When comparing with other methods in the UK Biobank experiments, due to the large number  
404 of test samples (60,000+), we are confident that the lasso and elastic-net methods are able to do  
405 significantly better than other methods. In fact, the standard error of  $R^2$  can be easily derived  
406 by the delta method, and the standard error of the AUC can be estimated and upper bounded by  
407  $1/(4 \min(m, n))$  (DeLong et al., 1988; Cortes and Mohri, 2005), where  $m, n$  represents the number  
408 of positive and negative samples. For height and BMI, it turns out that the standard errors are  
409 roughly 0.001, or 0.1%. For asthma and high cholesterol, considering the case rate around 12%,  
410 the standard errors can be upper bounded by 0.005, or 0.5%. Therefore, on height, BMI and  
411 asthma, the lasso and elastic net perform significantly better than the other methods, while on

412 high cholesterol, the Sequential LR and the relaxed lasso have competitive performance as well.

## 413 4 Materials and Methods

414 **Variants in the BASIL framework** Some other very useful components can be easily incorpo-  
415 rated into the BASIL framework. We will discuss debiasing using the relaxed lasso and the inclusion  
416 of adjustment covariates.

The lasso is known to shrink coefficients to exclude noise variables, but sometimes such shrink-  
age can degrade the predictive performance due to its effect on actual signal variables. Meinshausen  
(2007) introduces the relaxed lasso to correct for the potential over-shrinkage of the original lasso  
estimator. They propose a refitting step on the active set of the lasso solution with less regular-  
ization, while a common way of using it is to fit a standard OLS on the active set. The active set  
coefficients are then set to

$$\hat{\beta}_{\mathcal{A},\text{Relax}}(\lambda) = \underset{\beta_{\mathcal{A}} \in \mathbb{R}^{|\mathcal{A}|}}{\operatorname{argmin}} \|y - X_{\mathcal{A}}\beta_{\mathcal{A}}\|_2^2,$$

417 whereas the coefficients for the inactive set remain at 0. This refitting step can revert some of the  
418 shrinkage bias introduced by the vanilla lasso. It doesn't always reduce prediction error due to the  
419 accompanied increase in variance when there are many variables in the model or when the signals  
420 are weak. That being said, we can still insert a relaxed lasso step with little effort in our iterative  
421 procedure: once a valid lasso solution is found for a new  $\lambda$ , we may refit with OLS. As we iterate,  
422 we can monitor validation error for the lasso and the relaxed lasso. The relaxed lasso will generally  
423 end up choosing a smaller set of variables than the lasso solution in the optimal model.

424 In some applications such as GWAS, there may be confounding variables  $Z \in \mathbb{R}^{n \times q}$  that we  
425 want to adjust for in the model. Population stratification, defined as the existence of a systematic  
426 ancestry difference in the sample data, is one of the common factors in GWAS that can lead to  
427 spurious discoveries. This can be controlled for by including some leading principal components of  
428 the SNP matrix as variables in the regression (Price et al., 2006). In the presence of such variables,

429 we instead solve

$$(\hat{\alpha}(\lambda), \hat{\beta}(\lambda)) = \underset{\alpha \in \mathbb{R}^q, \beta \in \mathbb{R}^p}{\operatorname{argmin}} \frac{1}{2n} \|y - Z\alpha - X\beta\|_2^2 + \lambda \|\beta\|_1. \quad (7)$$

430 This variation can be easily handled with small changes in the algorithm. Instead of initializing  
431 the residual with the response  $y$ , we set  $r^{(0)}$  equal to the residual from the regression of  $y$  on the  
432 covariates. In the fitting step, in addition to the variables in the strong set, we include the covariates  
433 but leave their coefficients unpenalized as in (7). Notice that if we want to find relaxed lasso fit  
434 with the presence of adjustment covariates, we need to include those covariates in the OLS as well,  
435 i.e.,

$$(\hat{\alpha}_{\text{Relax}}(\lambda), \hat{\beta}_{\mathcal{A}, \text{Relax}}(\lambda)) = \underset{\alpha \in \mathbb{R}^q, \beta_{\mathcal{A}} \in \mathbb{R}^{|\mathcal{A}|}}{\operatorname{argmin}} \|y - Z\alpha - X_{\mathcal{A}}\beta_{\mathcal{A}}\|_2^2. \quad (8)$$

436

437 **UK Biobank experiment details** We focused on 337,199 White British unrelated individuals  
438 out of the full set of over 500,000 from the UK Biobank dataset (Bycroft et al., 2018) that satisfy  
439 the same set of population stratification criteria as in DeBoever et al. (2018): (1) self-reported  
440 White British ancestry, (2) used to compute principal components, (3) not marked as outliers for  
441 heterozygosity and missing rates, (4) do not show putative sex chromosome aneuploidy, and (5)  
442 have at most 10 putative third-degree relatives. These criteria are meant to reduce the effect of  
443 confoundedness and unreliable observations.

444 The number of samples is large in the UK Biobank dataset, so we can afford to set aside  
445 an independent validation set without resorting to the costly cross-validation to find an optimal  
446 regularization parameter. We also leave out a subset of observations as test set to evaluate the final  
447 model. In particular, we randomly partition the original dataset so that 60% is used for training,  
448 20% for validation and 20% for test. The lasso solution path is fit on the training set, whereas the  
449 desired regularization is selected on the validation set, and the resulting model is evaluated on the  
450 test set.

451 We are going to further discuss some details in our application that one might also encounter  
452 in practice. They include adjustment for confounders, missing value imputation and variable stan-

453 dardization in the algorithm.

454 In genetic studies, spurious associations are often found due to confounding factors. Among  
455 the others, one major source is the so-called population stratification (Patterson et al., 2006). To  
456 adjust for that effect, it is common is to introduce the top principal components and include them  
457 in the regression model. Therefore in the lasso method, we are going to solve (7) where in addition  
458 to the SNP matrix  $X$ , we let  $Z$  include covariates such as age, sex and the top 10 PCs of the SNP  
459 matrix.

460 Missing values are present in the dataset. As quality control normally done in genetics, we  
461 first discard observations whose phenotypic value of interest is not available. We further exclude  
462 variants whose missing rate is greater than 10% or the minor allele frequency (MAF) is less than  
463 0.1%, which results in around 685,000 SNPs for height. In particular, 685,362 for height, 685,371 for  
464 BMI, 685,357 for asthma and 685,357 for HC. The number varies because the criteria are evaluated  
465 on the subset of individuals whose phenotypic value is observed (after excluding the missing ones),  
466 which can be different across different phenotypes. For those remaining variants, mean imputation  
467 is conducted to fill the missing SNP values; that is, the missing values in every SNP are imputed  
468 with the mean observed level of that SNP in the population under study.

469 When it comes to the lasso fitting, there are some subtleties that can affect its variable selection  
470 and prediction performance. One of them is variable standardization. It is often a step done without  
471 much thought to deal with heterogeneity in variables so that they are treated fairly in the objective.  
472 However in our studies, standardization may create some undesired effect. To see this, notice that  
473 all the SNPs can only take values in 0, 1, 2 and NA — they are already on the same scale by  
474 nature. As we know, standardization would use the current standard deviation of each predictor  
475 as the divisor to equalize the variance across all predictors in the lasso fitting that follows. In this  
476 case, standardization would unintentionally inflate the magnitude of rare variants and give them  
477 an advantage in the selection process since their coefficients effectively receive less penalty after  
478 standardization. In Figure 6, we can see the distribution of standard deviation across all variants in  
479 our dataset. Hence, to avoid potential spurious findings, we choose not to standardize the variants  
480 in the experiments.





**Figure 6:** Histogram of the standard deviations of the SNPs. They are computed *after* mean imputation of the missing values because they would be the exact standardization factors to be used if the lasso were applied with variable standardization on the mean-imputed SNP matrix.

481 **Computational optimization in software implementation** Among the iterative steps in  
482 BASIL, screening and checking are where we need to deal with the full dataset. To deal with the  
483 memory bound, we can use memory-mapped I/O. In R, **bigmemory** (Kane et al., 2013) provides  
484 a convenient implementation for that purpose. That being said, we do not want to rely on that  
485 for intensive computation modules such as cyclic coordinate descent, because frequent visits to the  
486 on-disk data would still be slow. Instead, since the subset of strong variables would be small, we  
487 can afford to bring them to memory and do fast lasso fitting there. We only use the full memory-  
488 mapped dataset in KKT checking and screening. Moreover since checking in the current iteration  
489 can be done together with the screening in the next iteration, effectively only one expensive pass  
490 over the full dataset is needed every iteration.

In addition, we use a set of techniques to speed up the computation. First, the KKT check can be easily parallelized by splitting on the features when multi-core machines are available. The speedup of this part is immediate and (slightly less than) proportional to the number of cores available. Second, specific to the application, we exploit the fact that there are only 4 levels for each SNP

Multiplication Method	$n = 200, p = 800$	$n = 2000, p = 8000$
Standard	3.20	306.01
SNP-Optimized	1.32	130.21

**Table 3:** Timing performance (milliseconds) on multiplication of SNP matrix and residual matrix. The methods are all implemented in C++ and run on a Macbook with 2.9 GHz Intel Core i7 and 8 GB 1600 MHz DDR3.

value and design a faster inner product routine to replace normal float number multiplication in the KKT check step. In fact, given any SNP vector  $x \in \{0, 1, 2, \mu\}^n$  where  $\mu$  is the imputed value for the missing ones, we can write the dot product with a vector  $r \in \mathbb{R}^n$  as

$$x^\top r = \sum_{i=1}^n x_i r_i = 1 \cdot \sum_{i:x_i=1} r_i + 2 \cdot \sum_{i:x_i=2} r_i + \mu \cdot \sum_{i:x_i=\mu} r_i.$$

491 We see that the terms corresponding to 0 SNP value can be ignored because they don't contribute  
492 to the final result. This will significantly reduce the number of arithmetic operations needed to  
493 compute the inner product with rare variants. Further, we only need to set up 3 registers, each  
494 for one SNP value accumulating the corresponding terms in  $r$ . A series of multiplications is then  
495 converted to summations. In our UK Biobank studies, although the SNP matrix is not sparse  
496 enough to exploit sparse matrix representation, it still has around 70% 0's. We conduct a small  
497 experiment to compare the time needed to compute  $X^\top R$ , where  $X \in \{0, 1, 2, 3\}^{n \times p}$ ,  $R \in \mathbb{R}^{p \times k}$ .  
498 The proportions for the levels in  $X$  are about 70%, 10%, 10%, 10%, similar to the distribution of  
499 SNP levels in our study, and  $R$  resembles the residual matrix when checking the KKT condition.  
500 The number of residual vectors is  $k = 20$ . The mean time over 100 repetitions is shown in Table 3.

501 We implement the procedure with all the optimizations in an R package called **snpnet**, which is  
502 currently available at <https://github.com/junyangq/snpnet>. It assumes pgen file format (Chang  
503 et al., 2015) of the SNP matrix, fits the lasso solution path and allows early stopping if a validation  
504 dataset is provided. In order to achieve better efficiency, we suggest using **snpnet** together with  
505 **glmnetPlus**, a warm-started version of **glmnet**, which is currently available at <https://github.com/junyangq/glmnetPlus>. It allows one to provide a good initialization of the coefficients to fit  
506 part of the solution path instead of always starting from the all-zero solution by **glmnet**.  
507

508 **Related methods and packages** There are a number of existing screening rules for solving  
509 big lasso problems. Sobel et al. (2009) use a screened set to scale down the logistic lasso problem  
510 and check the KKT condition to validate the solution. Their focus, however, is on selecting a  
511 lasso model of particular size and only the initial screened set is expanded if the KKT condition is  
512 violated. In contrast, we are interested in finding the whole solution path (before overfitting). We  
513 adopt a sequential approach and keep updating the screened set at each iteration. This allows us  
514 to potentially keep the screened set small as we move along the solution path. Other rules include  
515 the SAFE rule (El Ghaoui et al., 2010), Sure Independence Screening (Fan and Lv, 2008), and the  
516 DPP and EDPP rules (Wang et al., 2015).

517 We expand the discussion on these screening rules a bit. Fan and Lv (2008) exploits marginal  
518 information of correlation to conduct screening but the focus there is not optimization algorithm.  
519 Most of the screening rules mentioned above (except for EDPP) use inner product with the current  
520 residual vector to measure the importance of each predictor at the next  $\lambda$  — those under a threshold  
521 can be ignored. The key difference across those rules is the threshold defined and whether the  
522 resulting discard is safe. If it is safe, one can guarantee that only one iteration is needed for each  $\lambda$   
523 value, compared with others that would need more rounds if an active variable was falsely discarded.  
524 Though the strong rules rarely make this mistake, safe screening is still a nice feature to have in  
525 single- $\lambda$  solutions. However, under the batch mode we consider due to the desire of reducing the  
526 number of full passes over the dataset, the advantage of safe threshold may not be as much. In  
527 fact, one way we might be able to leverage the safe rules in the batch mode is to first find out the  
528 set of candidate predictors for the several  $\lambda$  values up to  $\lambda_k$  we wish to solve in the next iteration  
529 based on the current inner products and the rules' safe threshold, and then solve the lasso for these  
530 parameters. Since these rules can often be conservative, we would then have strong incentive to  
531 solve for, say, one further  $\lambda$  value  $\lambda_{k+1}$  because if the current screening turns out to be a valid one  
532 as well, we will find one more lasso solution and move one step forward along the  $\lambda$  sequence we  
533 want to solve for. This can potentially save one iteration of the procedure and thus one expensive  
534 pass over the dataset. The only cost there is computing the lasso solution for one more  $\lambda_{k+1}$  and  
535 computing inner products with one more residual vector at  $\lambda_{k+1}$  (to check the KKT condition).

536 The latter can be done in the same pass as we compute inner products at  $\lambda_k$  for preparing the  
537 screening in the next iteration, and so no additional pass is needed. Thus under the batch mode,  
538 the property of safe screening may not be as important due to the incentive of aggressive model  
539 fitting. Nevertheless it would be interesting to see in the future EDPP-type batch screening. It  
540 uses inner products with a modification of the residual vector. Our algorithm still focuses of inner  
541 products with the vanilla residual vector.

542 To address the large-scale lasso problems, several packages have been developed such as **biglasso**  
543 (Zeng and Breheny, 2017), **bigstatsr** (Privé et al., 2018), **oem** (Huling and Qian, 2018) and the  
544 lasso routine from **PLINK** 1.9 (Chang et al., 2015).

545 Among them, **oem** specializes in tall data (big  $n$ ) and can be slow when  $p > n$ . In many real  
546 data applications including ours, the data are both large-sample and high-dimensional. However,  
547 we might still be able to use **oem** for the small lasso subroutine since a large number of variables  
548 have already been excluded. The other packages, **biglasso**, **bigstatsr**, **PLINK** 1.9, all provide  
549 efficient implementations of the pathwise coordinate descent with warm start. **PLINK** 1.9 is  
550 specifically developed for genetic datasets and is widely used in GWAS and research in population  
551 genetics. In **bigstatsr**, the **big\_spLinReg** function adapts from the **biglasso** function in **biglasso**  
552 and incorporates a Cross-Model Selection and Averaging (CMSA) procedure, which is a variant  
553 of cross-validation that saves computation by directly averaging the results from different folds  
554 instead of retraining the model at the chosen optimal parameter. They both use memory-mapping to  
555 process larger-than-RAM, on-disk datasets as if they were in memory, and based on that implement  
556 coordinate descent with strong rules and warm start.

557 The main difference between BASIL and the algorithm these packages use is that BASIL tries to  
558 solve a series of models every full scan of the dataset (at checking and screening) and thus effectively  
559 reduce the number of passes over the dataset. This difference may not be significant in small or  
560 moderate-sized problems, but can be critical in big data applications especially when the dataset  
561 cannot be fully loaded into the memory. A full scan of a larger-than-RAM dataset can incur a lot  
562 of swap-in/out between the memory and the disk, and thus a lot of disk I/O operations, which is  
563 known to be orders of magnitude slower than in-memory operations. Thus reducing the number of

564 full scans can greatly improve the overall performance of the algorithm.

565       Aside from potential efficiency consideration, all of those packages aforementioned have to re-  
566 implement a variety of features existent in many small-data solutions but for big-data context.  
567 Nevertheless, currently they don't provide as much functionality as needed in our real-data ap-  
568 plication. First, in the current implementations, **PLINK** 1.9 only supports the Gaussian family,  
569 **biglasso** and **bigstatsr** only supports the Gaussian and binomial families, whereas **snpnet** can  
570 easily extend to other regression families and already built in Gaussian, binomial and Cox fami-  
571 lies. Also, **biglasso**, **bigstatsr** and **PLINK** 1.9 all standardize the predictors beforehand, but in  
572 many applications such as our UK Biobank studies, it is more reasonable to leave the predictors  
573 unstandardized. In addition, it can take some effort to convert the data to the desired format by  
574 these packages. This would be a headache if the raw data is in some special format and one cannot  
575 afford to first convert the full dataset into an intermediate format for which a tool is provided to  
576 convert to the desired one by **biglasso** or **bigstatsr**. This can happen, for example, if the raw  
577 data is highly compressed in a special format. For the BED binary format we work with in our  
578 application, `readRAW_big.matrix` function from **BGData** can convert a raw file to a `big.matrix`  
579 object desired by **biglasso**, and `snp_readBed` function from **bigsnpr** (Privé et al., 2018) allows one  
580 to convert it to `FBM` object desired by **bigstatsr**. However, **bigsnpr** doesn't take input data that  
581 has any missing values, which can prevalent in an SNP matrix (as in our application). Although  
582 **PLINK** 1.9 works directly with the BED binary file, its lasso solver currently only supports the  
583 Gaussian family, and it doesn't return the full solution path. Instead it returns the solution at the  
584 smallest  $\lambda$  value computed and needs a good heritability estimate as input from the user, which  
585 may not be immediately available.

586       We summarize the main advantages of the BASIL algorithm:

- 587 • **Input data flexibility.** Our algorithm allows one to deal directly with any data type as  
588 long as the screening and checking steps are implemented, which is often very lightweight  
589 development work like matrix multiplication. This can be important in large-scale applications  
590 especially when the data is stored in a compressed format or a distributed way since then  
591 we would not need to unpack the full data and can conduct KKT check and screening on its

592 original format. Instead only a small screened subset of the data needs to be converted to the  
593 desired format by the lasso solver in the fitting step.

594 • **Model flexibility.** We can easily transfer the modeling flexibility provided by existing  
595 packages to the big data context, such as the options of standardization, sample weights,  
596 lower/upper coefficient limits and other families in generalized linear models provided by  
597 existing packages such as **glmnet**. This can be useful, for example, when we may not want to  
598 standardize predictors already in the same unit to avoid unintentionally different penalization  
599 of the predictors due to difference in their variance.

600 • **Effortless development.** The BASIL algorithm allows one to maximally reuse the existing  
601 lasso solutions for small or moderate-sized problems. The main extra work would be an  
602 implementation of batch screening and KKT check with respect to a particular data type.  
603 For example, in the **snpnet** package, we are able to quickly extend the in-memory **glmnet**  
604 solution to large-scale, ultrahigh-dimensional SNP data. Moreover, the existing convenient  
605 data interface provided by the **BEDMatrix** package further facilitates our implementation.

606 • **Computational efficiency.** Our design reduces the number of visits to the original data  
607 that sits on the disk, which is crucial to the overall efficiency as disk read can be orders of  
608 magnitude slower than reading from the RAM. The key to achieving this is to bring batches  
609 of promising variables into the main memory, hoping to find the lasso solutions for more than  
610 one  $\lambda$  value each iteration and check the KKT condition for those  $\lambda$  values in one pass of the  
611 entire dataset.

612 Lastly, we are going to provide some timing comparison with existing packages. As mentioned  
613 in previous sections, those packages provide different functionalities and have different restrictions  
614 on the dataset. For example, most of them (**biglasso**, **bigstatsr**) assume that there are no missing  
615 values, or the missing ones have already been imputed. In **bigsnpr**, for example, we shouldn't have  
616 SNPs with 0 MAF either. Some packages always standardize the variants before fitting the lasso.  
617 To provide a common playground, we create a synthetic dataset with no missing values, and follow  
618 a standardized lasso procedure in the fitting stage, simply to test the computation. The dataset has

R Package	Elapsed Time (minutes)
<b>bigstatsr</b> (Privé et al., 2018)	2.93 + 56.80
<b>bigstatsr</b> + CMSA (Privé et al., 2018)	2.93 + 101.75
<b>biglasso</b> (Zeng and Breheny, 2017)	4.55 + 54.27
<b>PLINK</b> (Chang et al., 2015)	53.52
<b>snpnet</b>	<b>44.79</b>

**Table 4:** Timing comparison on a synthetic dataset of size  $n = 50,000$  and  $p = 100,000$ . The time for **bigstatsr** and **biglasso** has two components: one for the conversion to the desired data type and the other for the actual computation. The experiments are all run with 16 cores and 64 GB memory.

50,000 samples and 100,000 variables, and each takes value in the SNP range, i.e., in 0, 1, or 2. We fit the first 50 lasso solutions along a prefix  $\lambda$  sequence that contains 100 initial  $\lambda$  values (like early stopping for most phenotypes). The total time spent is displayed in Table 4. For **bigstatsr**, we include two versions since it does cross-validation by default. In one version, we make it comply with our single train/val/test split, while in the other version, we use its default 10-fold cross-validation version — Cross-Model Selection and Averaging (CMSA). Notice that the final solution of iCMSA is different from the exact lasso solution on the full data because the returned coefficient vector is a linear combination of the coefficient vectors from the 10 folds rather than from a retrained model on the full data. We uses 128GB memory and 16 cores for the computation.

From the table, we see that **snpnet** is at about 20% faster than other packages concerned. The numbers before the “+” sign are the time spent on converting the raw data to the required data format by those packages. The second numbers are time spent on actual computation.

It is important to note though that the performance relies not only on the algorithm, but also heavily on the implementations. The other packages in comparison all have their major computation done with C++ or Fortran. Ours, for the purpose of meta algorithm where users can easily integrate with any lasso solver in R, still has a significant portion (the iterations) in R and multiple rounds of cross-language communication. That can degrade the timing performance to some degree. If there is further pursuit of speed performance, there is still space for improvement by more designated implementation.

## 638 Acknowledgements

639 We thank Balasubramanian Narasimhan for helpful discussion on the package development, Ken-  
640 neth Tay and the members of the Rivas lab for insightful feedback. J.Q. is partially supported by  
641 the Two Sigma Graduate Fellowship. Y.T. is supported by a Funai Overseas Scholarship from the  
642 Funai Foundation for Information Technology and the Stanford University School of Medicine.

643 M.A.R. is supported by Stanford University and a National Institute of Health center for Multi  
644 and Trans-ethnic Mapping of Mendelian and Complex Diseases grant (5U01 HG009080). This work  
645 was supported by National Human Genome Research Institute (NHGRI) of the National Institutes  
646 of Health (NIH) under awards R01HG010140. The content is solely the responsibility of the authors  
647 and does not necessarily represent the official views of the National Institutes of Health.

648 R.T. was partially supported by NIH grant 5R01 EB001988-16 and NSF grant 19 DMS1208164.

649 T.H. was partially supported by grant DMS-1407548 from the National Science Foundation, and  
650 grant 5R01 EB 001988-21 from the National Institutes of Health.

651 This research has been conducted using the UK Biobank Resource under application number  
652 24983. We thank all the participants in the study. The primary and processed data used to  
653 generate the analyses presented here are available in the UK Biobank access management system  
654 (<https://amsportal.ukbiobank.ac.uk/>) for application 24983, "Generating effective therapeutic  
655 hypotheses from genomic and hospital linkage data" ([http://www.ukbiobank.ac.uk/wp-content/  
656 uploads/2017/06/24983-Dr-Manuel-Rivas.pdf](http://www.ukbiobank.ac.uk/wp-content/uploads/2017/06/24983-Dr-Manuel-Rivas.pdf)), and the results are displayed in the Global  
657 Biobank Engine (<https://biobankengine.stanford.edu>).

658 Some of the computing for this project was performed on the Sherlock cluster. We would like  
659 to thank Stanford University and the Stanford Research Computing Center for providing compu-  
660 tational resources and support that contributed to these research results.

## 661 Author Contributions

662 **Conceptualization:** Junyang Qian, Trevor Hastie

663 **Data curation:** Yosuke Tanigawa, Matthew Aguirre, Manuel A. Rivas



664 **Formal Analysis:** Junyang Qian, Wenfei Du, Robert Tibshirani, Trevor Hastie  
665 **Funding Acquisition:** Robert Tibshirani, Manuel A. Rivas, Trevor Hastie  
666 **Methodology:** Junyang Qian, Trevor Hastie  
667 **Software:** Junyang Qian, Yosuke Tanigawa, Chris Chang  
668 **Supervision:** Robert Tibshirani, Manuel A. Rivas, Trevor Hastie  
669 **Validation:** Yosuke Tanigawa, Matthew Aguirre, Manuel A. Rivas  
670 **Visualization:** Junyang Qian, Wenfei Du  
671 **Writing - Original Draft:** Junyang Qian, Wenfei Du  
672 **Writing - Review & Editing:** Yosuke Tanigawa, Matthew Aguirre, Robert Tibshirani, Manuel  
673 A. Rivas, Trevor Hastie

## 674 **References**

675 Clare Bycroft, Colin Freeman, Desislava Petkova, Gavin Band, Lloyd T. Elliott, Kevin Sharp,  
676 Allan Motyer, Damjan Vukcevic, Olivier Delaneau, Jared O'Connell, Adrian Cortes, Samantha  
677 Welsh, Alan Young, Mark Effingham, Gil McVean, Stephen Leslie, Naomi Allen, Peter Donnelly,  
678 and Jonathan Marchini. The uk biobank resource with deep phenotyping and genomic data.  
679 *Nature*, 562(7726):203–209, 2018. ISSN 1476-4687. doi: 10.1038/s41586-018-0579-z. URL <https://doi.org/10.1038/s41586-018-0579-z>.  
680

681 Robert Tibshirani. Regression shrinkage and selection via the lasso. *Journal of the Royal Statistical*  
682 *Society. Series B (Methodological)*, 58(1):267–288, 1996. ISSN 00359246. URL <http://www.jstor.org/stable/2346178>.  
683

684 Jerome Friedman, Trevor Hastie, and Rob Tibshirani. Regularization paths for generalized linear  
685 models via coordinate descent, 2010a. ISSN 1548-7660. URL <https://www.jstatsoft.org/v033/i01>.  
686

687 Jerome Friedman, Trevor Hastie, and Robert Tibshirani. *The Elements of Statistical Learning:*

- 688 *Data Mining, Inference, and Prediction, 2nd Edition*. Springer series in statistics. Springer-  
689 Verlag, 2009. doi: 10.1007/978-0-387-84858-7.
- 690 Bradley Efron and Trevor Hastie. *Computer Age Statistical Inference: Algorithms, Evidence, and*  
691 *Data Science*, volume 5. Cambridge University Press, 2016.
- 692 Jeffrey Dean and Sanjay Ghemawat. Mapreduce: Simplified data processing on large clusters.  
693 *Commun. ACM*, 51(1):107–113, January 2008. ISSN 0001-0782. doi: 10.1145/1327452.1327492.  
694 URL <http://doi.acm.org/10.1145/1327452.1327492>.
- 695 Matei Zaharia, Mosharaf Chowdhury, Michael J. Franklin, Scott Shenker, and Ion Stoica. **Spark**:  
696 Cluster computing with working sets. In *Proceedings of the 2Nd USENIX Conference on Hot*  
697 *Topics in Cloud Computing*, HotCloud’10, pages 10–10, Berkeley, CA, USA, 2010. USENIX  
698 Association. URL <http://dl.acm.org/citation.cfm?id=1863103.1863113>.
- 699 Martín Abadi, Paul Barham, Jianmin Chen, Zhifeng Chen, Andy Davis, Jeffrey Dean, Matthieu  
700 Devin, Sanjay Ghemawat, Geoffrey Irving, Michael Isard, Manjunath Kudlur, Josh Levenberg,  
701 Rajat Monga, Sherry Moore, Derek G. Murray, Benoit Steiner, Paul Tucker, Vijay Vasudevan,  
702 Pete Warden, Martin Wicke, Yuan Yu, and Xiaoqiang Zheng. **TensorFlow**: A system for large-  
703 scale machine learning. In *Proceedings of the 12th USENIX Conference on Operating Systems De-*  
704 *sign and Implementation*, OSDI’16, pages 265–283, Berkeley, CA, USA, 2016. USENIX Associa-  
705 tion. ISBN 978-1-931971-33-1. URL <http://dl.acm.org/citation.cfm?id=3026877.3026899>.
- 706 R Core Team. *R: A Language and Environment for Statistical Computing*. R Foundation for  
707 Statistical Computing, Vienna, Austria, 2017. URL <https://www.R-project.org/>.
- 708 Patrick Breheny and Jian Huang. Coordinate descent algorithms for nonconvex penalized regression,  
709 with applications to biological feature selection. *The Annals of Applied Statistics*, 5(1):232–253,  
710 03 2011. doi: 10.1214/10-AOAS388. URL <https://doi.org/10.1214/10-AOAS388>.
- 711 Trevor Hastie. Statistical learning with big data. Presentation at Data Science at Stanford Seminar,  
712 2015.

- 713 Peter M. Visscher, Naomi R. Wray, Qian Zhang, Pamela Sklar, Mark I. McCarthy, Matthew A.  
714 Brown, and Jian Yang. 10 years of gwas discovery: Biology, function, and translation. *The*  
715 *American Journal of Human Genetics*, 101(1):5–22, 2017. ISSN 0002-9297. doi: 10.1016/j.ajhg.  
716 2017.06.005. URL <https://doi.org/10.1016/j.ajhg.2017.06.005>.
- 717 Christopher C Chang, Carson C Chow, Laurent CAM Tellier, Shashaank Vattikuti, Shaun M  
718 Purcell, and James J Lee. Second-generation PLINK: rising to the challenge of larger and richer  
719 datasets. *GigaScience*, 4(1), 02 2015. ISSN 2047-217X. doi: 10.1186/s13742-015-0047-8. URL  
720 <https://doi.org/10.1186/s13742-015-0047-8>.
- 721 Robert Tibshirani, Jacob Bien, Jerome Friedman, Trevor Hastie, Noah Simon, Jonathan Taylor,  
722 and Ryan J. Tibshirani. Strong rules for discarding predictors in lasso-type problems. *Journal*  
723 *of the Royal Statistical Society. Series B (Statistical Methodology)*, 74(2):245–266, 2012. ISSN  
724 13697412, 14679868. URL <http://www.jstor.org/stable/41430939>.
- 725 Stephen Boyd and Lieven Vandenberghe. *Convex Optimization*. Cambridge university press, 2004.
- 726 Jerome Friedman, Trevor Hastie, and Rob Tibshirani. Regularization paths for generalized linear  
727 models via coordinate descent. *Journal of Statistical Software, Articles*, 33(1):1–22, 2010b. ISSN  
728 1548-7660. doi: 10.18637/jss.v033.i01. URL <https://www.jstatsoft.org/v033/i01>.
- 729 D. R. Cox. Regression models and life-tables. *Journal of the Royal Statistical Society. Series B*  
730 *(Methodological)*, 34(2):187–220, 1972. ISSN 00359246. URL [http://www.jstor.org/stable/](http://www.jstor.org/stable/2985181)  
731 [2985181](http://www.jstor.org/stable/2985181).
- 732 Ruilin Li, Christopher Chang, Johanne Marie Justesen, Yosuke Tanigawa, Junyang Qian, Trevor  
733 Hastie, Manuel A. Rivas, and Robert Tibshirani. Fast lasso method for large-scale and ultrahigh-  
734 dimensional cox model with applications to uk biobank. *bioRxiv*, 2020. doi: 10.1101/2020.01.20.  
735 913194. URL <https://www.biorxiv.org/content/early/2020/01/21/2020.01.20.913194>.
- 736 Hui Zou and Trevor Hastie. Regularization and variable selection via the elastic net. *Journal of the*  
737 *Royal Statistical Society: Series B (Statistical Methodology)*, 67(2):301–320, 2005. doi: 10.1111/j.

738 1467-9868.2005.00503.x. URL <https://rss.onlinelibrary.wiley.com/doi/abs/10.1111/j.>

739 1467-9868.2005.00503.x.

740 Louis Lello, Steven G. Avery, Laurent Tellier, Ana I. Vazquez, Gustavo de los Campos, and Stephen  
741 D. H. Hsu. Accurate genomic prediction of human height. *Genetics*, 210(2):477–497, 2018. ISSN  
742 0016-6731. doi: 10.1534/genetics.118.301267. URL [http://www.genetics.org/content/210/](http://www.genetics.org/content/210/2/477)  
743 [2/477](http://www.genetics.org/content/210/2/477).

744 Christopher DeBoever, Yosuke Tanigawa, Malene E. Lindholm, Greg McInnes, Adam Lavertu,  
745 Erik Ingelsson, Chris Chang, Euan A. Ashley, Carlos D. Bustamante, Mark J. Daly, and  
746 Manuel A. Rivas. Medical relevance of protein-truncating variants across 337,205 individuals  
747 in the uk biobank study. *Nature Communications*, 9(1):1612, 2018. ISSN 2041-1723. doi:  
748 10.1038/s41467-018-03910-9. URL <https://doi.org/10.1038/s41467-018-03910-9>.

749 Herman Wold. Soft modelling by latent variables: The non-linear iterative partial least squares  
750 (nipals) approach. *Journal of Applied Probability*, 12(S1):117?142, 1975. doi: 10.1017/  
751 S0021900200047604.

752 Nicolai Meinshausen. Relaxed lasso. *Computational Statistics & Data Analysis*, 52(1):374 – 393,  
753 2007. ISSN 0167-9473. doi: <https://doi.org/10.1016/j.csda.2006.12.019>. URL [http://www.](http://www.sciencedirect.com/science/article/pii/S0167947306004956)  
754 [sciencedirect.com/science/article/pii/S0167947306004956](http://www.sciencedirect.com/science/article/pii/S0167947306004956).

755 Tian Ge, Chia-Yen Chen, Yang Ni, Yen-Chen Anne Feng, and Jordan W Smoller. Polygenic  
756 prediction via bayesian regression and continuous shrinkage priors. *Nature Communications*, 10  
757 (1):1–10, 2019.

758 Luke R Lloyd-Jones, Jian Zeng, Julia Sidorenko, Loïc Yengo, Gerhard Moser, Kathryn E Kemper,  
759 Huanwei Wang, Zhili Zheng, Reedik Magi, Tonu Esko, et al. Improved polygenic prediction by  
760 bayesian multiple regression on summary statistics. *Nature Communications*, 10(1):1–11, 2019.

761 Jian Zeng, Ronald De Vlaming, Yang Wu, Matthew R Robinson, Luke R Lloyd-Jones, Loic Yengo,  
762 Chloe X Yap, Angli Xue, Julia Sidorenko, Allan F McRae, et al. Signatures of negative selection  
763 in the genetic architecture of human complex traits. *Nature Genetics*, 50(5):746–753, 2018.

- 764 Yosuke Tanigawa, Jiehan Li, Johanne M Justesen, Heiko Horn, Matthew Aguirre, Christopher  
765 DeBoever, Chris Chang, Balasubramanian Narasimhan, Kasper Lage, Trevor Hastie, et al. Com-  
766 ponents of genetic associations across 2,138 phenotypes in the uk biobank highlight adipocyte  
767 biology. *Nature communications*, 10(1):1–14, 2019.
- 768 Karri Silventoinen, Sampo Sammalisto, Markus Perola, Dorret I. Boomsma, Belinda K. Cornes,  
769 Chayna Davis, Leo Dunkel, Marlies de Lange, Jennifer R. Harris, Jacob V.B. Hjelmberg, and  
770 et al. Heritability of adult body height: A comparative study of twin cohorts in eight countries.  
771 *Twin Research*, 6(5):399–408, 2003. doi: 10.1375/twin.6.5.399.
- 772 Peter M Visscher, Sarah E Medland, Manuel A. R Ferreira, Katherine I Morley, Gu Zhu, Belinda K  
773 Cornes, Grant W Montgomery, and Nicholas G Martin. Assumption-free estimation of heritability  
774 from genome-wide identity-by-descent sharing between full siblings. *PLOS Genetics*, 2(3):1–10,  
775 03 2006. doi: 10.1371/journal.pgen.0020041. URL [https://doi.org/10.1371/journal.pgen.](https://doi.org/10.1371/journal.pgen.0020041)  
776 [0020041](https://doi.org/10.1371/journal.pgen.0020041).
- 777 Peter M. Visscher, Brian McEvoy, and Jian Yang. From galton to gwas: Quantitative genetics of  
778 human height. *Genetics Research*, 92(5-6):371–379, 2010. doi: 10.1017/S0016672310000571.
- 779 Noah Zaitlen, Peter Kraft, Nick Patterson, Bogdan Pasaniuc, Gaurav Bhatia, Samuela Pollack,  
780 and Alkes L. Price. Using extended genealogy to estimate components of heritability for 23  
781 quantitative and dichotomous traits. *PLOS Genetics*, 9(5):1–11, 05 2013. doi: 10.1371/journal.  
782 [pgen.1003520](https://doi.org/10.1371/journal.pgen.1003520). URL <https://doi.org/10.1371/journal.pgen.1003520>.
- 783 Gibran Hemani, Jian Yang, Anna Vinkhuyzen, Joseph E Powell, Gonneke Willemsen, Jouke-Jan  
784 Hottenga, Abdel Abdellaoui, Massimo Mangino, Ana M Valdes, Sarah E Medland, Pamela A  
785 Madden, Andrew C Heath, Anjali K Henders, Dale R Nyholt, Eco J C. de Geus, Patrik K E.  
786 Magnusson, Erik Ingelsson, Grant W Montgomery, Timothy D Spector, Dorret I Boomsma,  
787 Nancy L Pedersen, Nicholas G Martin, and Peter M Visscher. Inference of the genetic architecture  
788 underlying bmi and height with the use of 20,240 sibling pairs. *The American Journal of Human*

789 *Genetics*, 93(5):865–875, 2013. ISSN 0002-9297. doi: 10.1016/j.ajhg.2013.10.005. URL <https://doi.org/10.1016/j.ajhg.2013.10.005>.  
790

791 Jian Yang, Beben Benyamin, Brian P. McEvoy, Scott Gordon, Anjali K. Henders, Dale R. Nyholt,  
792 Pamela A. Madden, Andrew C. Heath, Nicholas G. Martin, Grant W. Montgomery, Michael E.  
793 Goddard, and Peter M. Visscher. Common snps explain a large proportion of the heritability for  
794 human height. *Nature Genetics*, 42:565, 2010. doi: 10.1038/ng.608. URL <https://doi.org/10.1038/ng.608>.  
795

796 Jian Yang, Andrew Bakshi, Zhihong Zhu, Gibran Hemani, Anna A. E. Vinkhuyzen, Sang Hong  
797 Lee, et al. Genetic variance estimation with imputed variants finds negligible missing heritability  
798 for human height and body mass index. *Nature Genetics*, 47:1114, 2015. doi: 10.1038/ng.3390.  
799 URL <https://doi.org/10.1038/ng.3390>.

800 Hana Lango Allen, Karol Estrada, Guillaume Lettre, Sonja I. Berndt, Michael N. Weedon, Fernando  
801 Rivadeneira, et al. Hundreds of variants clustered in genomic loci and biological pathways affect  
802 human height. *Nature*, 467:832, 2010. doi: 10.1038/nature09410. URL <https://doi.org/10.1038/nature09410>.  
803

804 Andrew R. Wood, Tonu Esko, Jian Yang, Sailaja Vedantam, Tune H. Pers, Stefan Gustafsson,  
805 et al. Defining the role of common variation in the genomic and biological architecture of adult  
806 human height. *Nature Genetics*, 46:1173, 2014. doi: 10.1038/ng.3097. URL <https://doi.org/10.1038/ng.3097>.  
807

808 Eirini Marouli, Mariaelisa Graff, Carolina Medina-Gomez, Ken Sin Lo, Andrew R. Wood, Troels R.  
809 Kjaer, et al. Rare and low-frequency coding variants alter human adult height. *Nature*, 542:186,  
810 2017. doi: 10.1038/nature21039. URL <https://doi.org/10.1038/nature21039>.

811 Neal Parikh and Stephen Boyd. Proximal algorithms. *Foundations and Trends in Optimization*, 1  
812 (3):127–239, January 2014. ISSN 2167-3888. doi: 10.1561/2400000003. URL <http://dx.doi.org.stanford.idm.oclc.org/10.1561/2400000003>.  
813

- 814 Lin Xiao. Dual averaging methods for regularized stochastic learning and online optimization.  
815 *Journal of Machine Learning Research*, 11(Oct):2543–2596, 2010.
- 816 J. C. Duchi, A. Agarwal, and M. J. Wainwright. Dual averaging for distributed optimization:  
817 Convergence analysis and network scaling. *IEEE Transactions on Automatic Control*, 57(3):  
818 592–606, March 2012. ISSN 0018-9286. doi: 10.1109/TAC.2011.2161027.
- 819 Peter J. Bickel, Ya’acov Ritov, and Alexandre B. Tsybakov. Simultaneous analysis of lasso and  
820 dantzig selector. *Ann. Statist.*, 37(4):1705–1732, 08 2009. doi: 10.1214/08-AOS620. URL <https://doi.org/10.1214/08-AOS620>.
- 822 Peng Zhao and Bin Yu. On model selection consistency of lasso. *Journal of Machine learning*  
823 *research*, 7(Nov):2541–2563, 2006.
- 824 Elizabeth R. DeLong, David M. DeLong, and Daniel L. Clarke-Pearson. Comparing the areas  
825 under two or more correlated receiver operating characteristic curves: A nonparametric approach.  
826 *Biometrics*, 44(3):837–845, 1988. ISSN 0006341X, 15410420. URL <http://www.jstor.org/stable/2531595>.
- 828 Corinna Cortes and Mehryar Mohri. Confidence intervals for the area under the roc curve. In  
829 *Advances in Neural Information Processing Systems*, pages 305–312, 2005.
- 830 Alkes L. Price, Nick J. Patterson, Robert M. Plenge, Michael E. Weinblatt, Nancy A. Shadick, and  
831 David Reich. Principal components analysis corrects for stratification in genome-wide association  
832 studies. *Nature Genetics*, 38:904, 2006. doi: 10.1038/ng1847. URL <https://doi.org/10.1038/ng1847>.
- 834 Nick Patterson, Alkes L Price, and David Reich. Population structure and eigenanalysis. *PLOS*  
835 *Genetics*, 2(12):1–20, 12 2006. doi: 10.1371/journal.pgen.0020190. URL <https://doi.org/10.1371/journal.pgen.0020190>.
- 837 Michael J. Kane, John Emerson, and Stephen Weston. Scalable strategies for computing with

- 838 massive data. *Journal of Statistical Software*, 55(14):1–19, 2013. URL <http://www.jstatsoft.org/v55/i14/>.
- 839
- 840 Eric Sobel, Kenneth Lange, Tong Tong Wu, Trevor Hastie, and Yi Fang Chen. Genome-Wide  
841 Association Analysis by Lasso Penalized Logistic Regression. *Bioinformatics*, 25(6):714–721, 01  
842 2009. ISSN 1367-4803. doi: 10.1093/bioinformatics/btp041. URL [https://doi.org/10.1093/](https://doi.org/10.1093/bioinformatics/btp041)  
843 [bioinformatics/btp041](https://doi.org/10.1093/bioinformatics/btp041).
- 844 Laurent El Ghaoui, Vivian Viallon, and Tarek Rabbani. Safe feature elimination for the lasso and  
845 sparse supervised learning problems. *arXiv preprint arXiv:1009.4219*, 2010.
- 846 Jianqing Fan and Jinchi Lv. Sure independence screening for ultrahigh dimensional feature space.  
847 *Journal of the Royal Statistical Society: Series B (Statistical Methodology)*, 70(5):849–911, 2008.  
848 doi: 10.1111/j.1467-9868.2008.00674.x. URL [https://rss.onlinelibrary.wiley.com/doi/](https://rss.onlinelibrary.wiley.com/doi/abs/10.1111/j.1467-9868.2008.00674.x)  
849 [abs/10.1111/j.1467-9868.2008.00674.x](https://rss.onlinelibrary.wiley.com/doi/abs/10.1111/j.1467-9868.2008.00674.x).
- 850 Jie Wang, Peter Wonka, and Jieping Ye. Lasso screening rules via dual polytope projection. *Journal of Machine Learning Research*, 16:1063–1101, 2015. URL [http://jmlr.org/papers/v16/](http://jmlr.org/papers/v16/wang15a.html)  
851 [wang15a.html](http://jmlr.org/papers/v16/wang15a.html).
- 852
- 853 Yaohui Zeng and Patrick Breheny. The **biglasso** package: A memory-and computation-efficient  
854 solver for lasso model fitting with big data in R. *arXiv preprint arXiv:1701.05936*, 2017.
- 855 Florian Privé, Michael G B Blum, Hugues Aschard, and Andrey Ziyatdinov. Efficient Analysis of  
856 Large-Scale Genome-Wide Data with Two R packages: **bigstatsr** and **bigsnpr**. *Bioinformatics*,  
857 34(16):2781–2787, 03 2018. ISSN 1367-4803. doi: 10.1093/bioinformatics/bty185.
- 858 Jared D Huling and Peter ZG Qian. Fast penalized regression and cross validation for tall data  
859 with the **oem** package. *arXiv preprint arXiv:1801.09661*, 2018.
- 860 Elizabeth K. Speliotes, Cristen J. Willer, Sonja I. Berndt, Keri L. Monda, Gudmar Thorleifsson,  
861 Anne U. Jackson, et al. Association analyses of 249,796 individuals reveal 18 new loci associated



862 with body mass index. *Nature Genetics*, 42:937, 2010. doi: 10.1038/ng.686. URL <https://doi.org/10.1038/ng.686>.  
863

864 Adam E. Locke, Bratati Kahali, Sonja I. Berndt, Anne E. Justice, Tune H. Pers, Felix R. Day, Corey  
865 Powell, et al. Genetic studies of body mass index yield new insights for obesity biology. *Nature*,  
866 518:197, 2015. doi: 10.1038/nature14177. URL <https://doi.org/10.1038/nature14177>.

867 Stephen D. Turner. **qqman**: An R package for visualizing gwas results using q-q and manhattan  
868 plots. *Journal of Open Source Software*, 3(25):731, 2018. doi: 10.21105/joss.00731.

## 869 **A Results for Additional Phenotypes**

### 870 **A.1 Body Mass Index (BMI)**

871 BMI is another polygenic trait that is widely studied. Like height, it is heritable and easily mea-  
872 sured. It is also a trait of interest, since obesity is a risk factor for diseases such as type 2 diabetes  
873 and cardiovascular disease. Recent studies estimate heritability at 0.42 (Zaitlen et al., 2013; Hemani  
874 et al., 2013) and 27% of the variance can be explained using a genomic model (Yang et al., 2015).  
875 We expect the heritability to be lower than that for height, since intuitively speaking, one com-  
876 ponent of the body mass, weight, should heavily depend on environmental factors, for example,  
877 individual’s lifestyle. From GWAS studies, 97 associated loci have been identified, but they only  
878 account for 2.7% of the variance (Speliotes et al., 2010; Locke et al., 2015). Although the estimates  
879 of heritability are not precise, there may be more missing heritability for BMI than for height. We  
880 also find lower  $R^2$  values using the lasso. The results are summarized in Table 5. The  $R^2$  curves  
881 for the lasso and the relaxed lasso are shown in Figure 7. From the table, we see that more than  
882 26,000 variants are selected by the lasso to attain an  $R^2$  greater than 10%. In contrast, the relaxed  
883 lasso and the sequential linear regression use around one-tenths of the variables, and end up with  
884 degraded predictive performance both at around 5%. From Figure 8, we see further evidence that  
885 the actual BMI is of high variability and hard to predict with the lasso model — the correlation  
886 between the predicted value and the actual value is 0.3256. From the residual histogram on the  
887 right, we also see the distribution is skewed to the right, suggesting a number of exceedingly high  
888 observed values than the ones predicted by the model. Nevertheless, we are able to predict BMI  
889 within 9 kg/m<sup>2</sup> about 95% of the time.

### 890 **A.2 Asthma**

891 Asthma is a common respiratory disease characterized by inflammation of airways in the lungs and  
892 difficulty breathing. It is another complex, polygenic trait that is associated with both genetic  
893 and environmental factors. Our results are summarized in Table 6. The AUC curves for the lasso  
894 and the relaxed lasso are shown in Figure 9. In addition, for each test sample, we compute the

Model	Form	$R^2_{\text{train}}$	$R^2_{\text{val}}$	$R^2_{\text{test}}$	Size
(1)	Age + Sex	0.0092	0.0089	0.0083	2
(2)	Age + Sex + 10 PCs	0.0104	0.0103	0.0099	12
(3)	(2) + Single SNP	0.0134	0.0128	0.0124	13
(4)	(2) + 10K Combined	0.0384	0.0195	0.0210	10,012
(5)	(2) + 100K Combined	0.1307	0.0064	0.0093	100,012
(6)	Sequential LR	0.0865	0.0385	0.0395	2,012
(7)	Lasso	0.3196	0.1017	<b>0.1052</b>	26,060
(8)	Relaxed Lasso	0.1609	0.0504	0.0537	2,585
(9)	Elastic Net	0.3923	0.1040	0.1071	29,548
(10)	PRS-CS	0.0490	—	0.0315	148,052
(11)	SBayesR	0.0231	—	0.0139	658,693

**Table 5:**  $R^2$  values for BMI. For lasso and relaxed lasso, the chosen model is based on maximum  $R^2$  on the validation set. Model (3) to (8) each includes Model (2) plus their own specification as stated in the Form column. The validation results for PRS-CS and SBayesR are not available because we used a combined training and validation set for training.

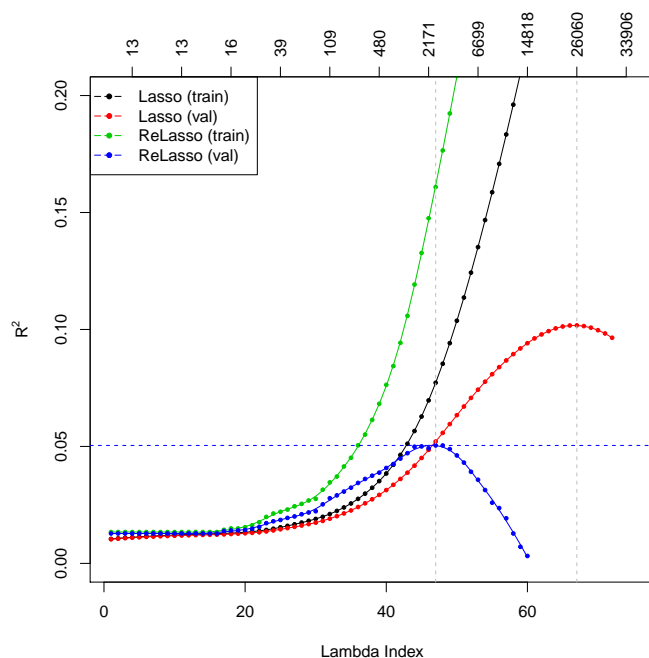


**Figure 7:**  $R^2$  plot for BMI. The top axis shows the number of active variables in the model.

895 percentile of its predicted score/probability among the entire test cohort, and create box plots of  
 896 such percentiles separately for the control group and the case group. We see on the left of Figure 10  
 897 that there is a significant overlap between the box plots of the two groups, suggesting that asthma

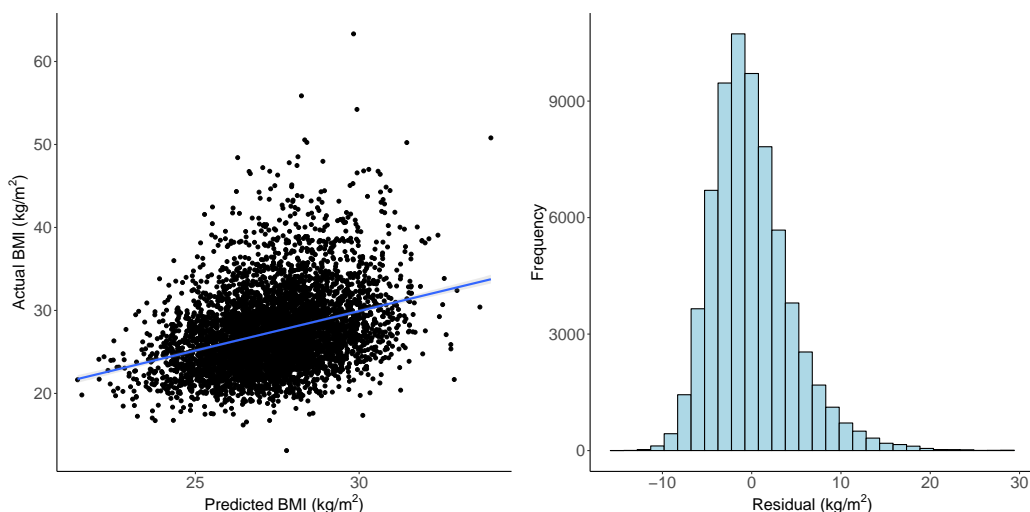


**Figure 8:** Left: actual BMI versus predicted BMI on 5000 random samples from the test set. The correlation between actual BMI and predicted BMI is 0.3256. Right: residuals of lasso prediction for BMI. Standard deviation of the residual is 4.51 kg/m<sup>2</sup>.

Model	Form	AUC <sub>train</sub>	AUC <sub>val</sub>	AUC <sub>test</sub>	Size
(1)	Age + Sex	0.5293	0.5297	0.5320	2
(2)	Age + Sex + 10 PCs	0.5342	0.5344	0.5367	12
(3)	(2) + Single SNP	0.5463	0.5476	0.5454	13
(4)	(2) + 10K Combined	0.5783	0.5580	0.5531	10,012
(5)	(2) + 100K Combined	0.6884	0.5644	0.5580	100,012
(6)	Sequential LR	0.6601	0.5883	0.5884	2,012
(7)	Lasso	0.7692	0.6159	<b>0.6126</b>	5,936
(8)	Relaxed Lasso	0.6747	0.5988	0.5955	621
(9)	Elastic Net	0.7803	0.6167	0.6131	7,799
(10)	PRS-CS	0.6300	–	0.5837	148,052
(11)	SBayesR	0.6340	–	0.5491	658,693

**Table 6:** AUC values for asthma. For lasso and relaxed lasso, the chosen model is based on maximum AUC on the validation set. Model (3) to (8) each includes Model (2) plus their own specification as stated in the Form column. The validation results for PRS-CS and SBayesR are not available because we used a combined training and validation set for training.

898 is difficult to predict. This can also be seen from the AUC value and the ROC curve in Figure 13.  
 899 That being said, the multivariate lasso still does much better than the baseline model and the  
 900 strongest univariate model. On the right of Figure 10, we stratify the prediction percentile into 10  
 901 bins, and compute the overall prevalence within each bin. We observe a clear upward trend that  
 902 provides further evidence that we manage to capture some genetic signal there.

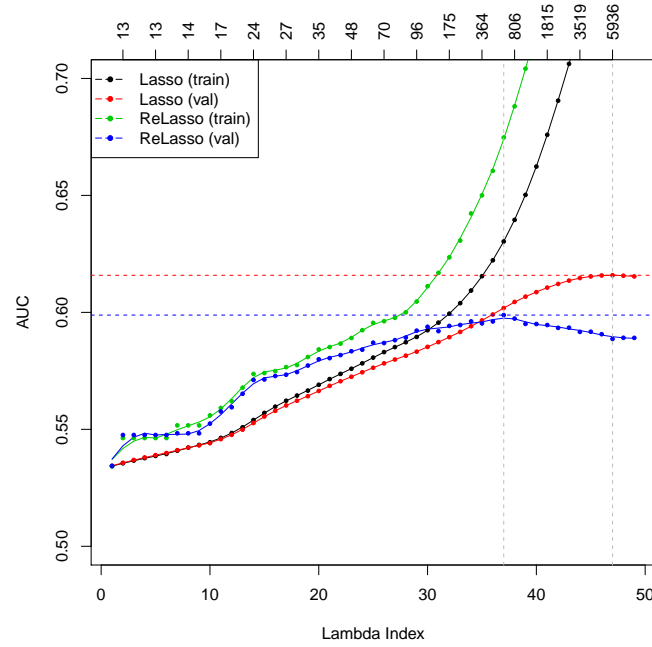


**Figure 9:** AUC plot for asthma. The top axis shows the number of active variables in the model.

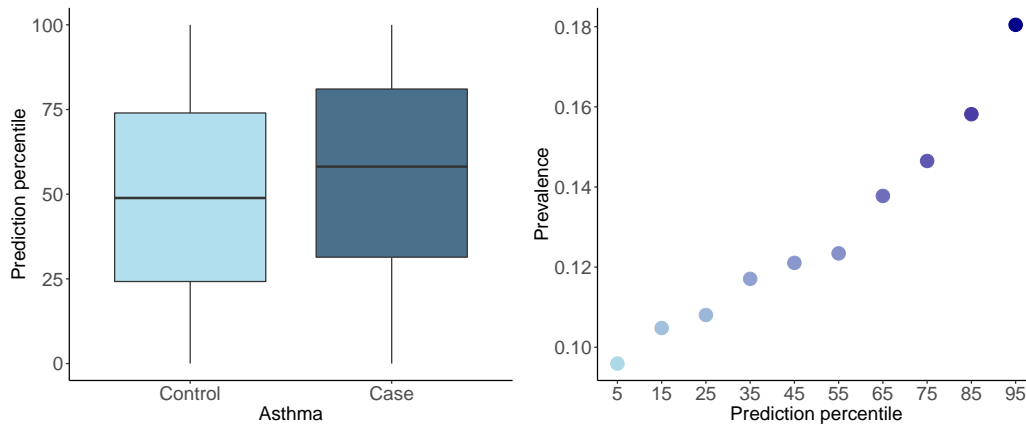


**Figure 10:** Results for asthma based on the best lasso model. Left: box plot of the percentile of the linear prediction score among cases versus controls. Right: the stratified prevalence across different percentile bins based on the predicted scores by the optimal lasso.

### 903 A.3 High Cholesterol

904 High cholesterol is characterized by high amounts of cholesterol present in the blood and is a risk

Model	Form	AUC <sub>train</sub>	AUC <sub>val</sub>	AUC <sub>test</sub>	Size
(1)	Age + Sex	0.6918	0.6952	0.6883	2
(2)	Age + Sex + 10 PCs	0.6927	0.6959	0.6889	12
(3)	(2) + Single SNP	0.6963	0.6982	0.6921	13
(4)	(2) + 10K Combined	0.7402	0.6956	0.6880	10,012
(5)	(2) + 100K Combined	0.8518	0.6607	0.6547	100,012
(6)	Sequential LR	0.7540	0.7167	0.7137	1,012
(7)	Lasso	0.7832	0.7259	<b>0.7191</b>	1,371
(8)	Relaxed Lasso	0.7273	0.7220	0.7166	239
(9)	Elastic Net	0.7830	0.7259	0.7190	4,277
(10)	PRS-CS	0.7166	–	0.7027	148,052
(11)	SBayesR	0.7148	–	0.6953	658,693

**Table 7:** AUC values for high cholesterol. For lasso and relaxed lasso, the chosen model is based on maximum AUC on the validation set. Model (3) to (8) each includes Model (2) plus their own specification as stated in the Form column. The validation results for PRS-CS and SBayesR are not available because we used a combined training and validation set for training.

905 factor for cardiovascular disease. It is highly heritable and may be polygenic. Our results are  
906 summarized in Table 7. The AUC curves for the lasso and the relaxed lasso are shown in Figure 11.  
907 Similarly the ROC curve for the best lasso model is shown in Figure 13, and box plots for the  
908 two groups and a stratified prevalence plot are shown in Figure 12. We see that the distributions  
909 of predictions made on non-HC individuals and on HC individuals are clearly different from each  
910 other, suggesting good classification results. That is reflected in the AUC measure listed in the  
911 table. Nevertheless, it is not much better than the result of the base model including only covariates  
912 age and sex.

## 913 B Manhattan Plots

914 The Manhattan plots in Figure 14 (generated using the **qqman** package (Turner, 2018)) show the  
915 magnitude of the univariate  $p$ -values and the size of the lasso coefficients for each gene for the  
916 two quantitative traits and two binary traits. The coefficients are plotted for the model with the  
917 optimal  $R^2$  value on the validation set. The variants highlighted in green in both plots are those  
918 that have coefficient magnitudes above the 99th percentile of all coefficient magnitudes for the trait.  
919 The horizontal line in the  $p$ -value plot is plotted at the genome-wide Bonferroni corrected  $p$ -value

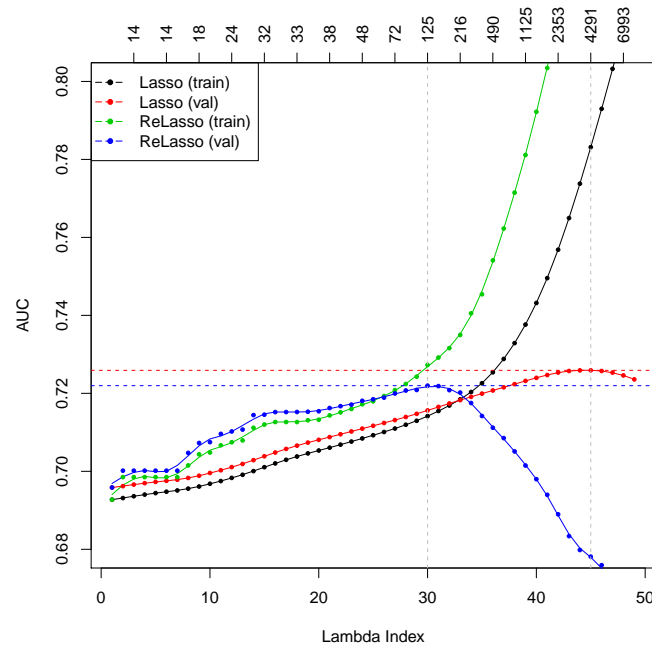


**Figure 11:** AUC plot for high cholesterol. The top axis shows the number of active variables in the model.

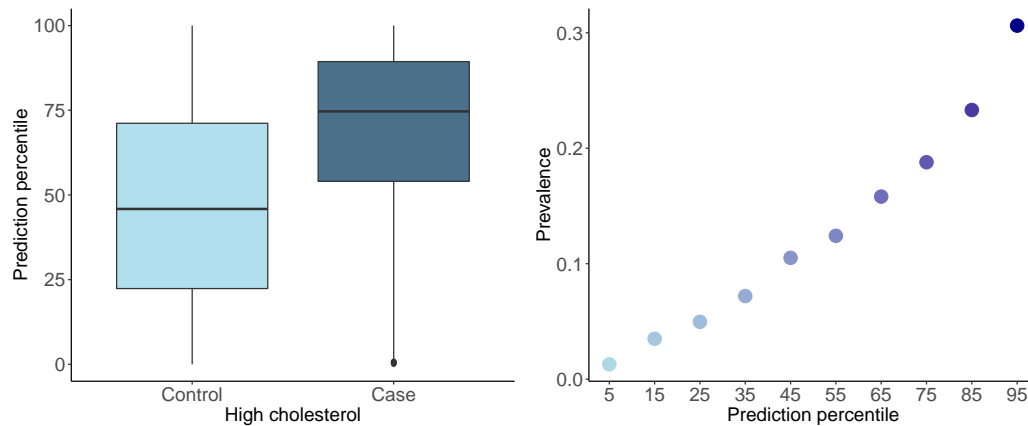


**Figure 12:** Results for high cholesterol based on the best lasso model. Left: box plot of the percentile of the linear prediction score among cases versus controls. Right: the stratified prevalence across different percentile bins based on the predicted scores by the optimal lasso.

920 threshold  $5 \times 10^{-8}$ . There are two main points we would like to highlight:

- 921 • The lasso manages to capture significant univariate predictors in each genetic region. Due
- 922 to possible correlation it does not pick up the variants with similarly small  $p$ -values located

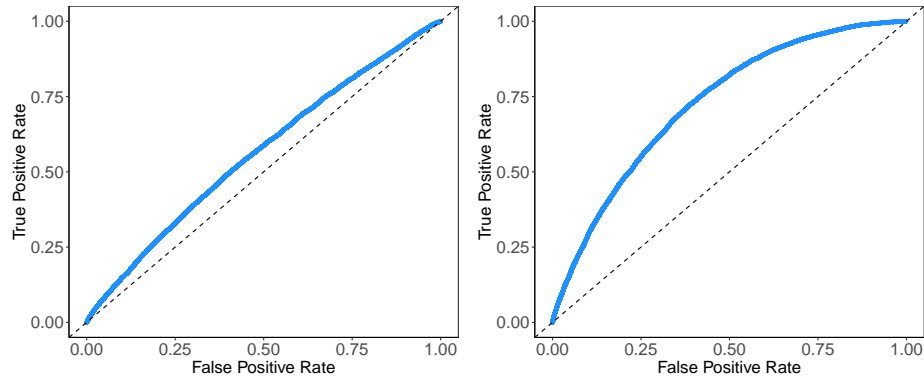


**Figure 13:** ROC curves. Left: asthma. Right: high cholesterol.

923 nearby.

- 924 • Some of the variants with weak univariate signals are also identified and turn out to be crucial  
925 to the predictive performance of the lasso.

926 For the two qualitative traits plotted in Figure 15, there are fewer  $p$ -values above the threshold,  
927 and many of the significant ones are located close to each other. The size of the lasso fit is corre-  
928 spondingly smaller, and the large coefficients pick up the important locations as before. However,  
929 the nonzero coefficients are still spread across the whole genome.



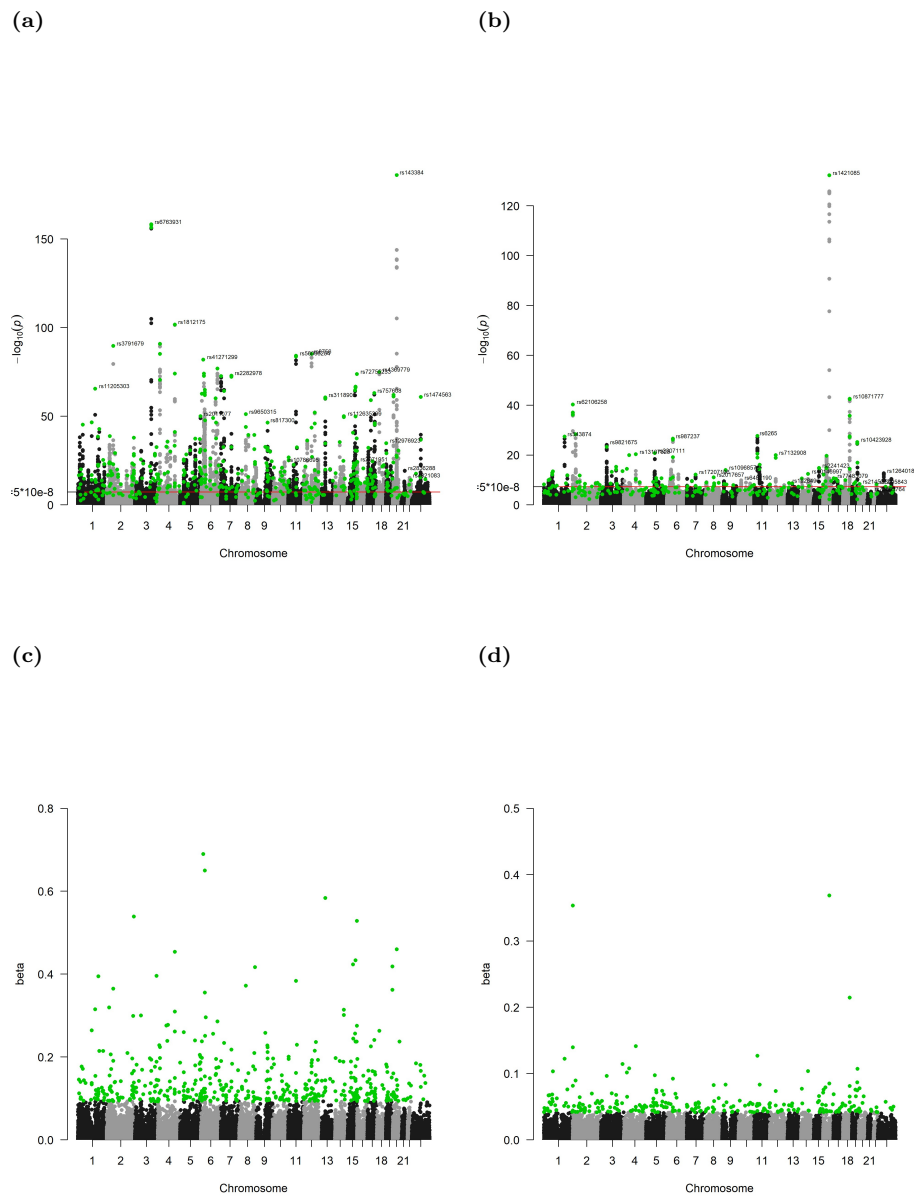


**Figure 14:** Manhattan plots of the univariate  $p$ -values and lasso coefficients for height (a, c) and BMI (b, d). The vertical axis of the  $p$ -value plots shows  $-\log_{10}(p)$  for each SNP, while the vertical axis of the coefficient plots shows the magnitude of the coefficients from **snpnet**. The SNPs with relatively large lasso coefficients are highlighted in green. The red horizontal line on the  $p$ -value plot represents a reference level of  $p = 5 \times 10^{-8}$ .

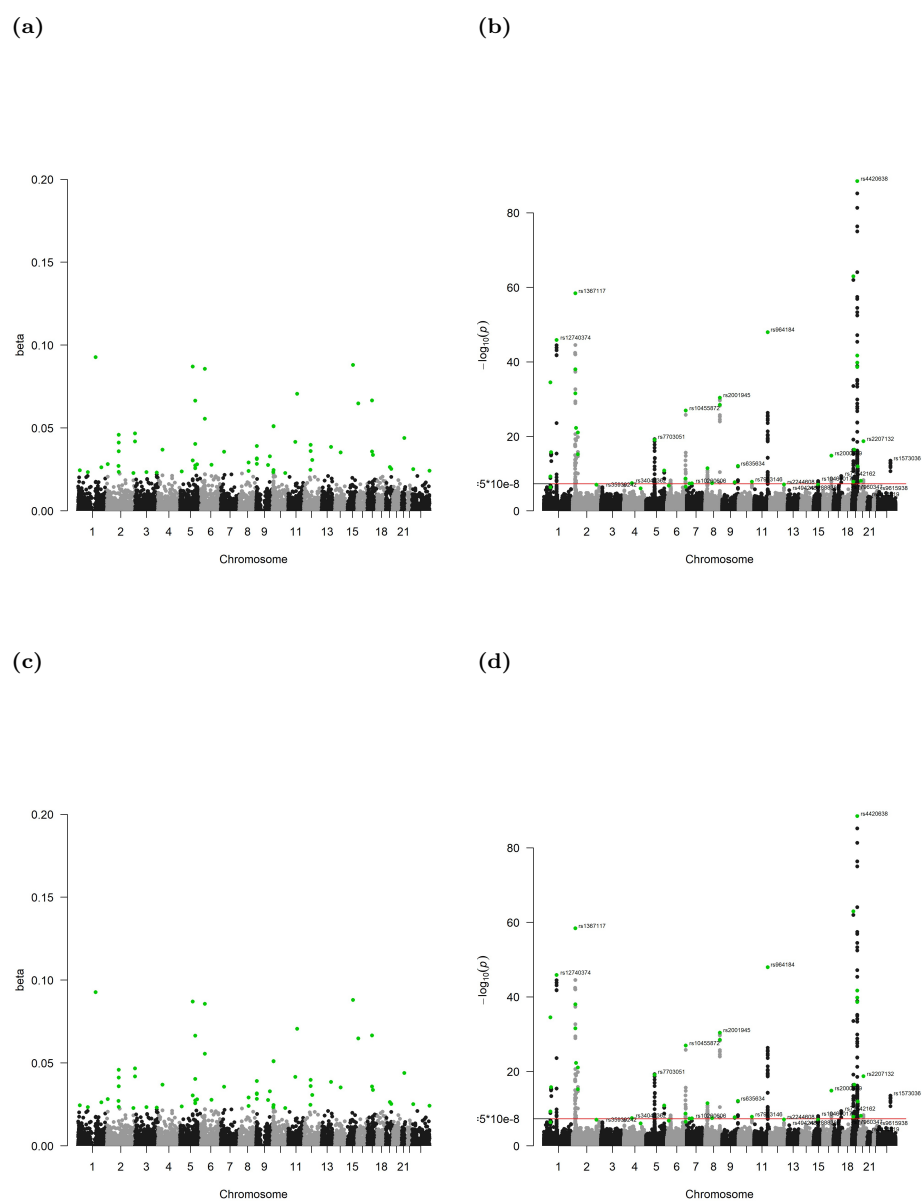


**Figure 15:** Manhattan plots of the univariate  $p$ -values and lasso coefficients for asthma (a, c) and high cholesterol (b, d). The vertical axis of the  $p$ -value plots shows  $-\log_{10}(p)$  for each SNP, while the vertical axis of the coefficient plots shows the magnitude of the coefficients from **snpnet**. The SNPs with relatively large lasso coefficients are highlighted in green. The red horizontal line on the  $p$ -value plot represents a reference level of  $p = 5 \times 10^{-8}$ .